

## REVIEW ARTICLE

## Surface-initiated polymerization from carbon nanotubes: strategies and perspectives

Cite this: *Chem. Soc. Rev.*, 2013, **42**, 677

Georgios Sakellariou,<sup>\*a</sup> Dimitrios Priftis<sup>a</sup> and Durairaj Baskaran<sup>†\*b</sup>

Carbon nanotubes (CNTs) represent one of the most promising materials in nanoscience today, with their unique electronic, chemical and mechanical properties. Strong van der Waals interactions and poor solubility greatly affect their potential for applications in various fields. In the past decade, great efforts have been undertaken to modify CNTs into organophilic material *via* covalent and non-covalent grafting strategies. This review focuses on advances in various strategies used for the surface initiated polymerization and provides perspectives on grafting polymers covalently from CNTs.

Received 27th June 2012

DOI: 10.1039/c2cs35226e

[www.rsc.org/csr](http://www.rsc.org/csr)

## 1 Introduction

Carbon nanotubes (CNTs), first reported by Iijima in 1991,<sup>1</sup> possess attractive properties such as high surface area, high aspect ratio ( $\sim 1000$ ), very high flexibility,<sup>2</sup> and low mass density.<sup>3</sup> Furthermore, they exhibit a unique combination of electrical, thermal and mechanical properties such as high tensile

strength ( $\sim 70$  GPa), elastic modulus ( $\sim 200$  MPa), and Young's modulus ( $\sim 1.5$  TPa).<sup>2,3</sup> These extraordinary properties of CNTs have attracted a great interest in academic and industrial research. Developments in the synthesis and characterization of CNTs over the past few decades have broadened the scope for their applications in a wide range of technologies.<sup>2,3</sup>

Single-wall and multi-wall carbon nanotubes (SWNTs and MWNTs) are considered as prototype one-dimensional solid quantum wires. Ultra-high strength materials, sensors, bio-medical devices, photovoltaic cells, and batteries are some areas, where CNTs find potential applications. However, the application of CNTs, in general, requires dispersion in polymers, organic-, and aqueous media. The presence of a hexagonal  $sp^2$  carbon network in CNTs renders a strong van der Waals interaction.

<sup>a</sup> Department of Chemistry, University of Athens, 15771 Panepistimiopolis Zografou, Athens, Greece. E-mail: [gsakellariou@chem.uoa.gr](mailto:gsakellariou@chem.uoa.gr)

<sup>b</sup> Department of Chemistry, University of Tennessee, Knoxville, TN 37996, USA

<sup>c</sup> AZ Electronic Materials USA Corp., 70 Meister Avenue, Somerville, New Jersey 08876, USA. E-mail: [durairaj.baskaran@az-em.com](mailto:durairaj.baskaran@az-em.com)

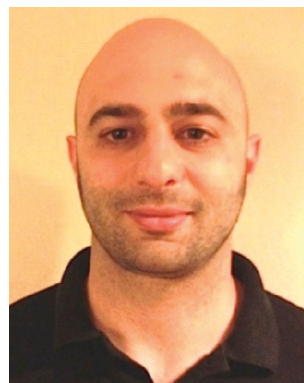
<sup>†</sup> Current address: AZ Electronic Materials USA Corp., 70 Meister Avenue, Somerville, New Jersey 08876, USA. E-mail: [durairaj.baskaran@az-em.com](mailto:durairaj.baskaran@az-em.com)



**Georgios Sakellariou**

*Georgios Sakellariou received his BSc (1999) and PhD (2003) in chemistry from the University of Athens, Greece. He then moved to the University of Tennessee, where he worked as a postdoctoral researcher in the group of Prof. Jimmy W. Mays (2004–2006). He was appointed as lecturer at the Department of Chemistry, University of Athens in 2010. Current recent interests in his group include the synthesis of polymers with*

*complex macromolecular architectures, surface-initiated polymerizations and the solution and bulk properties of nano-materials.*



**Dimitrios Priftis**

*Dimitrios Priftis received a BSc in chemistry from the Aristotle University of Thessaloniki in 2004. He then moved to the University of Athens where he obtained a MSc (2006) and a PhD (2009) in polymer chemistry (for his work on polymer functionalization of carbon nanotubes) under the supervision of Prof. N. Hadjichristidis. In 2010, he joined Prof. M. Tirrell's group as a postdoctoral researcher (focusing on the design, development and*

*study of the behavior of polyelectrolyte complexes) initially at the University of California, Berkeley and currently at the Institute for Molecular Engineering at the University of Chicago.*

A combination of a large surface area and a high aspect ratio with attractive van der Waal interaction forces CNTs to exist in aggregated bundles and thus, often, difficult to mix with organic materials. The problem associated with aggregation has to be circumvented in order to homogeneously disperse CNTs in solution and blend with polymers. One way to suppress the overwarming van der Waals interaction is to modify the surface of the carbon nanotubes through chemical reactions with small molecules or polymers.

### 1.1 Need for chemical functionalization of CNTs

One of the potential applications of CNTs is their use as nanofibers in designing novel ultrahigh strength polymer composites. A good interfacial adhesion between the CNTs and the polymer is essential for an efficient load transfer in composite application. However, aggregation of CNTs dominates in the preparation of polymer nanocomposites. Aggregation of CNTs significantly affects mechanical and electronic properties of the polymer nanocomposites due to microphase segregation, inefficient load transfer, and limited percolation network formation. Thus, the attractive properties of carbon nanotubes can only be realized if aggregation is suppressed and molecular dispersion is achieved.<sup>4</sup> Moreover, molecular dispersion of CNTs in solution as well as in polymer is essential to obtain uniform coating on any substrate for application related to the development of detectors and devices. Therefore, a complete dispersion of CNTs is crucial in producing novel ultrahigh strength polymer composites and coatings. A stumbling block in developing polymer-carbon nanotube composites is the poor dispersion and inefficient control of CNTs orientation in the polymer matrix.<sup>5</sup> Thus, small molecules and polymers are grafted to modify the surface of the CNTs in order to achieve an enhanced dispersion.

Polymer functionalized CNTs have also opened a new promising road for targeted-drug delivery, designed to selectively

direct the therapeutic treatment towards the tumour.<sup>6</sup> Carbon nanotubes functionalized with biocompatible polymers, like poly(ethyleneoxide) or polyesters, display low toxicity and are not immunogenic. Thus, functionalized CNTs hold great potential in the field of nanobiotechnology and nanomedicine.

### 1.2 Complexity associated with grafting procedures

Several methods for the functionalization of CNTs with organic moieties have been developed through covalent and non-covalent reactions. The non-covalent functionalization exploits  $\pi$ - $\pi$ , ionic, and H-bonding interactions with CNTs using suitable organic molecules such as pyrene, poly(*meta*-phenylene vinylene), poly(styrene sulfonate), cyclodextrin, *etc.* These molecules adsorb onto the electron rich CNTs and wrap around them *via* weak secondary interactions. On the other hand, covalent modification involves direct reactions with either the  $sp^2$  carbons of CNTs or the residual carboxylic acid on the CNTs.

Various oxidative purification processes of CNTs introduce acid along with small amount of anhydride, ether, and alcohol functionalities. These functional groups are used for attaching organic moieties on the CNTs. However, the chemical functionalization of CNTs is a complex process as the tubes are insoluble in organic medium and the reaction must be conducted either in bulk or in a heterogeneous medium. As the chemical reaction on CNTs is heterogeneous, it will be incomplete and will produce multiple products with a variable degrees of functionalization. More importantly CNTs are not monodisperse, in diameter and length, and even a small difference in the degree of functionalization with organic compounds introduces solubility variations in the functionalized CNTs. As a result, the availability of the tubes that are partially solvated for further reaction is affected. Thus, it is difficult to control the efficiency and the specificity of organic reactions with CNTs, especially with respect to the placement of functional groups and the degree of functionalization. Nevertheless, the attachment of organic moieties on the  $sp^2$  carbons of CNTs introduces an organophilic character, helps dispersing them in organic solvents and therefore, significantly increases the potential applications.

The first polymer nanocomposite, using CNTs as filler, was reported in 1994 by Ajayan *et al.*<sup>7</sup> To ensure a homogeneous dispersion of CNTs in polymer matrices, the surface of the CNTs needs to be grafted with chemically compatible polymers. Covalent grafting of polymers onto CNTs can be performed *via* *grafting to* and *grafting from* strategies. The residual carboxylic acid or chemically reacted functional groups on the walls and at the ends of CNTs were used for grafting applications. It is known that grafting  $\omega$ -functionalized high molecular weight polymers *via* a *grafting to* method is inefficient due to entropy-penalty associated with the conformation of macromolecules. Thus, for grafting high molecular weight polymers, the *grafting to* method is not a preferred one. The *grafting from* strategy otherwise called surface initiated polymerization (SIP) is the most promising one, since it provides control over the functionality, density, thickness, composition and architecture of the grafted polymers. Herein, we focus on the covalent grafting of polymers from SWNTs and MWNTs and discuss different polymerization methods that



**Durairaj Baskaran**

*Durairaj Baskaran received his MSc in applied chemistry from the Anna University, Chennai. He attended graduate school at the National Chemical Laboratory, India and University of Mainz, Germany. After his PhD (University of Pune, India, 1996), he worked as a senior scientist at the National Chemical Laboratory for several years before joining the University of Tennessee. His research interests are in the area of living anionic*

*polymerization and controlled radical polymerization focused on synthesis and characterization of architecturally controlled polymers, functionalization of carbon nanotubes, and nanocomposites. He has published over 80 research articles, several patents and co-edited a book.*

have been used for grafting polymers *via* SIP. The advantages and limitations of SIP from CNTs are being critically reviewed.

## 2 Surface-initiated polymerization (SIP) from CNTs

Introduction of an appropriate functional group is a first step towards growing polymers from the surface of CNTs. The functional group is then modified with a potential initiator moiety for the controlled vinyl polymerization. The introduction of functional groups is generally performed *via* the *grafting to* method, which has problems associated with adsorption, and entropic constrain. However, conformation related entropic constrain would not complicate the efficiency of grafting reactions, if the chemical reagent involved is a small molecule. Adsorption of unreacted small molecules can be easily removed *via* employing a thorough solvent washing procedure.

Acid groups are generated on the walls and tips of CNTs from oxidization procedures employed for recovery and purification. Generally, the acid groups are used for the attachment of an initiator *via* esterification or amidation (Scheme 1).<sup>8,9</sup> Direct reactions such as 1,3-dipolar, Diels–Alder [4 + 2], and nitrene [2 + 1] cycloadditions on the  $sp^2$  carbons of CNTs are other common methods used for the introduction of functional groups that allow the attachment of potential initiator moieties (Scheme 1).

As the CNTs are not monodisperse in terms of their length and diameter, any chemical reaction on CNTs will give a complex mixture of products, depending on the reaction efficiency. Therefore, the attachment of an initiator on the CNTs is a random process and the grafting density of polymers grown from them will also be inhomogeneous. Thus, the individual CNTs will have

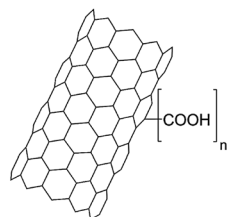
different properties, associated with the degree of functionalization. For example, the tubes with a higher polymer graft-density will be soluble in organic solvents whereas the tubes with a lower graft-density will be insoluble. Obviously, it is not possible to precisely control the number of grafted polymers and their molecular weight on an individual nanotube using SIP, considering a broad molecular distribution of the CNTs and the heterogeneous nature of the grafting reaction. This complexity has to be considered when analyzing the CNTs grafted with polymers. The advent of controlled and living polymerization techniques enables successful SIP from CNTs. In fact, the use of controlled or living polymerization is a prerequisite for grafting polymers from CNTs as the initiator is covalently anchored on the CNTs and polymer can propagate from it without undergoing termination and transfer reactions.

All known types of the living and controlled polymerization techniques have been utilized for grafting polymers covalently onto CNTs. The polymerization methods that have been employed are atom transfer radical polymerization (ATRP), reversible addition fragmentation chain transfer polymerization (RAFT), nitroxide mediated radical polymerization (NMRP), anionic polymerization, and ring-opening polymerization (ROP). In this review, we present the strategies and perspectives of covalent grafting of polymers from CNTs using controlled polymerization techniques.

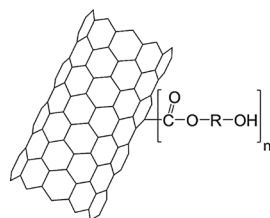
### 2.1 Application of vinyl polymerizations

**2.1.1 Atom transfer radical polymerization (ATRP).** ATRP is one of the best methods in reversible-deactivation radical polymerization that provides well-defined vinyl polymers.<sup>10–12</sup> ATRP is the most widely used method for covalent grafting of

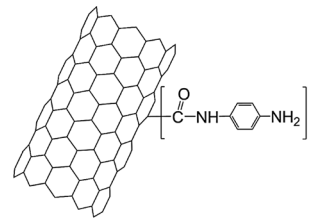
#### 1) CNTs-(COOH)<sub>n</sub> and derivatives



Oxidation

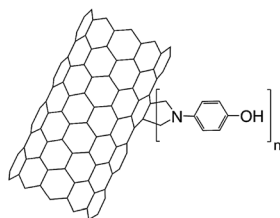


Esterification

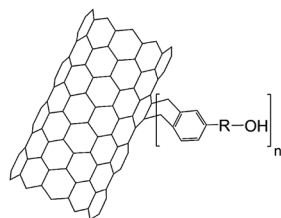


Amidation

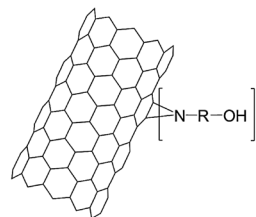
#### 2) CNTs-(OH)<sub>n</sub>



1,3-Dipolar cycloaddition



Diels-Alder [4 + 2] cycloaddition



[2 + 1] Cycloaddition

**Scheme 1** Functional groups of CNTs introduced *via* various chemical reactions for attachment of potential initiator moieties. Notation for a number of functional groups grafted to the different  $sp^2$  carbons on the CNTs is indicated as a group within a bracket with a number “*n*” for clarity.

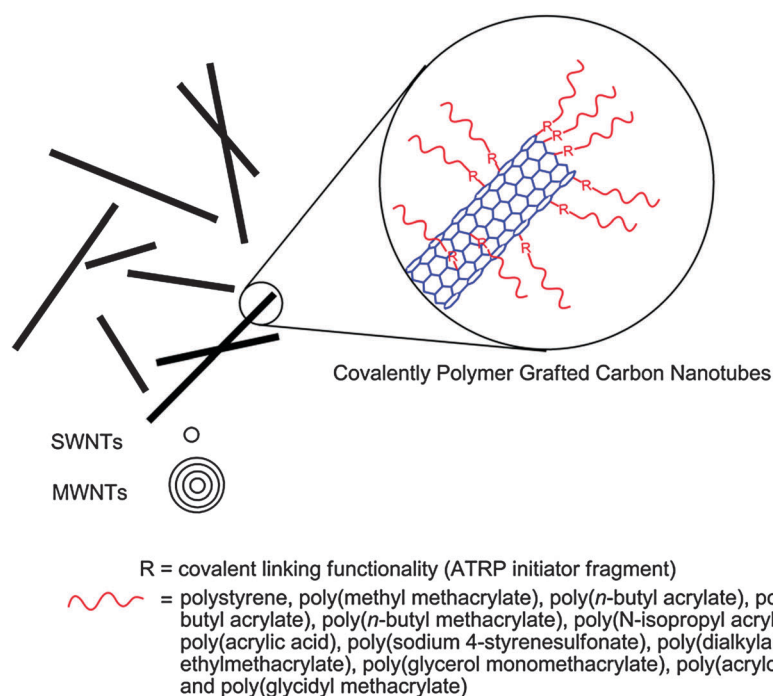
polymers from surfaces including CNTs.<sup>13–15</sup> This method requires attachment of alkyl halides suitable for initiation of vinyl monomers onto the CNTs. The living/controlled nature of this method and the variety of monomers that can be polymerized have led many groups to use ATRP in their studies for growing homopolymers, diblock copolymers and hyperbranched polymers from CNTs.

The first few attempts to initiate vinyl monomers using ATRP from CNTs were reported simultaneously by four independent groups, Adronov, Ford, Gao and Baskaran.<sup>16–19</sup> The main strategy involves the functionalization of CNTs to introduce hydroxyl or carboxylic acid groups. Subsequently, the hydroxyl or carboxylic acid groups on the CNTs are reacted with suitable reagents to convert into initiators for ATRP. Several types of vinyl polymers that have been grown *via* surface initiated ATRP are given in Scheme 2.

Types of initiators attached to the surface of the CNTs and their use in SIP are summarized in Scheme 3. Adronov's group<sup>16</sup> used a 1,3-dipolar cycloaddition to functionalize SWNTs with phenol followed by esterification with 2-bromoisobutryl bromide to generate ATRP initiator on the surface of SWNTs and polymerized MMA and *t*-BA. The grafted polymers were cleaved from the SWNTs and analyzed by Size Exclusion Chromatography (SEC) in order to understand the surface initiated polymerization process. While the mass of the nanotube sample increased during the reaction in a linear function, the molecular weights of the grafted polymers were non-linear. As the amount of initiator on the tubes was not determined, the verification of control over the process was difficult. However, high molecular weight polymers were grafted in all cases even at a short polymerization time, in addition the obtained polydispersity indices were higher than 1.6. Their attempt to further

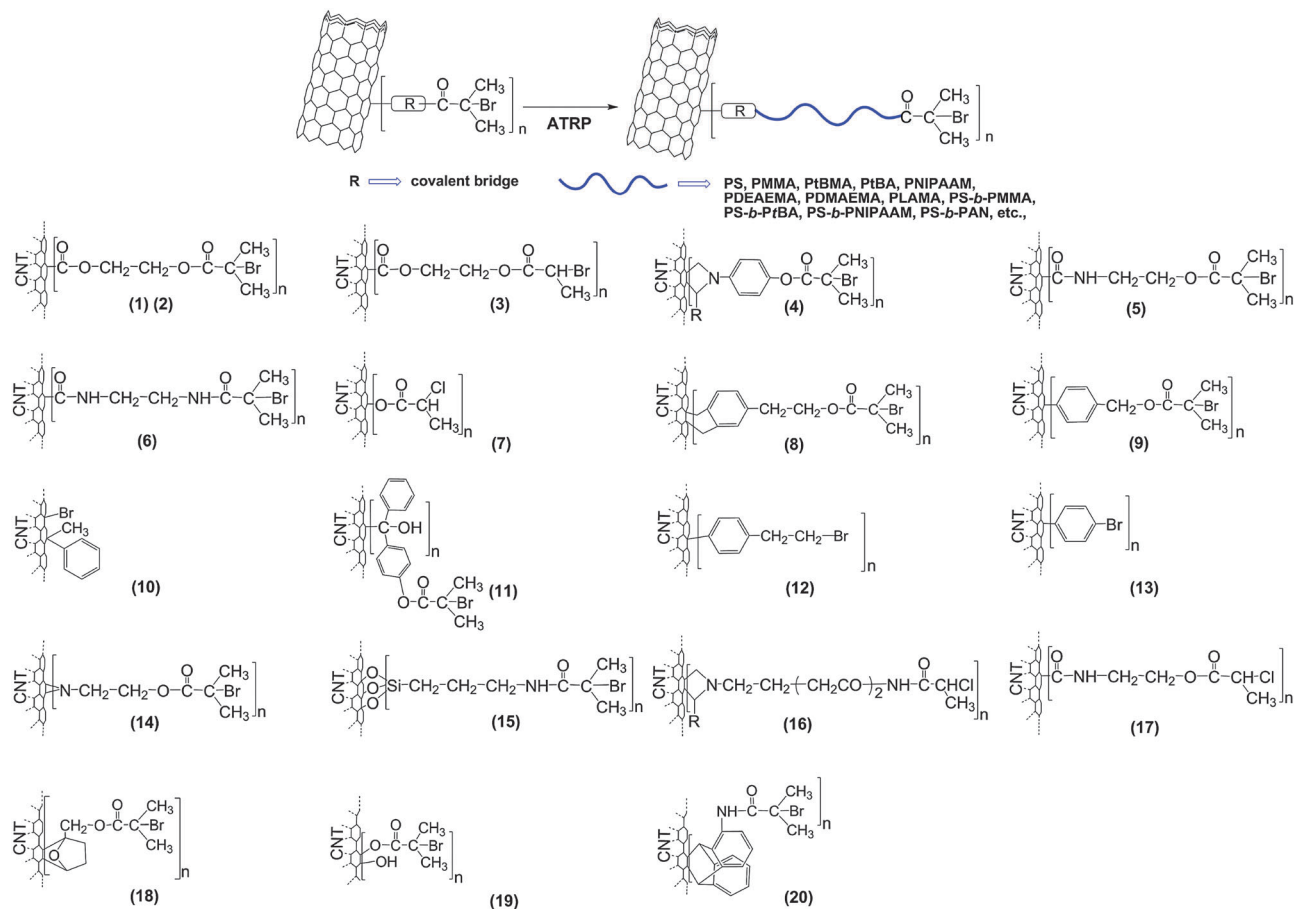
increase the molecular weight of the grafted polymer using a monomer resumption method failed, which showed that the polymerization did not proceed in a controlled manner. In order to control the polymerization, they introduced a small amount of sacrificial initiator, which was unsuccessful as it consumed all the monomer without an appreciable mass increase in the recovered nanotubes. The authors attributed this behavior to an extremely low concentration of the grafted initiator on the tubes, which could not compete with the free initiator when present in the reaction mixture. Furthermore, a control experiment performed in the presence of unfunctionalized SWNTs, under a similar condition, produced a polymer with a higher molecular weight than the expected one (based on monomer feed) and exhibited with a high polydispersity index ( $\sim 2.5$ ). It was concluded that the presence of SWNTs interferes with the polymerization and also act as radical scavenger causing an uncontrolled polymerization. The reason for obtaining a broad molecular weight distribution (MWD) is not clearly stated. The presence of covalently grafted PMMA on SWNTs (SWNTs-*g*-PMMA) was confirmed using solid-state nuclear magnetic resonance spectroscopy (NMR) and scanning tunneling microscopy (STM).<sup>20</sup>

Carboxylic acid groups introduced during the oxidative purification of CNTs have been used for surface modification in several reports.<sup>17–19,21</sup> Ford and co-workers<sup>17</sup> reacted hydroxyethyl-2-bromopropionate with the acid groups of the SWNTs (SWNTs-(COOH)<sub>*x*</sub>) and used them for the surface initiated ATRP of *n*-butyl methacrylate (*n*-BMA) and styrene (S). The amount of initiator on the surface of SWNTs was determined through thermogravimetric analysis (TGA). The study revealed that the SIP was controlled *via* the addition of a small amount of sacrificial initiator into the heterogeneous polymerization medium. It was



**Scheme 2** Various vinyl polymers grafted from CNTs *via* surface initiated ATRP.





**Scheme 3** General methodology for covalently connecting ATRP initiators and surface initiated grafting of various vinyl polymers. Notation for a number of functional groups grafted to the different  $\text{sp}^2$  carbons on the CNTs is indicated as a group within a bracket with a number “ $n$ ” for clarity.

shown that the molecular weight of the grafted chains was adjustable through control of the monomer/initiator ratio or the monomer conversion (Fig. 1). The molecular characteristics (molecular weight and polydispersity index) of the free *Pn*BMA chains were very similar to the grafted ones, in contrast to the results presented by Adronov and co-workers.<sup>16</sup> The authors claimed that the solution polymerization proceeded in a controlled manner, and the weight of the grafted polymer increased linearly with the molecular weight of the free *Pn*BMA chains (Fig. 1). However, the rate of propagation of the polymer anchored on the tubes will be dependent on the length and the diameter of the tubes. As a result the shorter tubes disperse in the reaction medium as soon as a few wt% of polymer grow from them. Thus, the molecular weight control in SIP from CNTs using ATRP will not be precise as in the case of a homogeneous solution ATRP. They have also synthesized SWNT-*g*-PS using a similar strategy and showed that the polymer grafted SWNTs exhibit increased solubility in several organic solvents.<sup>22</sup> Subsequently, Ford and co-workers demonstrated the synthesis of different types of polymers conjugated with SWNTs that are suitable for specific applications such as photovoltaics,<sup>23–25</sup> since the photoexcitation of these nanohybrids afforded radical ion pairs with long life times.

Gao *et al.*<sup>18</sup> and Baskaran *et al.*<sup>19</sup> independently reported the surface initiated ATRP using acid functionalized MWNTs. The

acid groups were modified into ATRP initiator through esterification with hydroxyethyl-2-bromoisobutyrate. Gao *et al.*<sup>18</sup> showed that the thickness of the polymer layer covering the MWNTs as well as the weight fraction of the grafted PMMA increased with increasing concentration of MMA in the reaction. Baskaran *et al.*<sup>19</sup> polymerized S and MMA using a similar approach and produced MWNTs-*g*-PMMA and MWNTs-*g*-PS with inhomogeneous coating on the surface. Non-uniform distribution of the initiator on the MWNTs was responsible for the discontinuous coverage of polymer over the carbon nanotubes. The SIP was performed without the sacrificial initiator with a very low attached initiator concentration ( $10^{-6}$ – $10^{-7}$  moles  $\text{mg}^{-1}$  carbon) and up to 70 wt% polymers and copolymers were grown on the MWNTs (Fig. 2a). They used the grafted PS chain-end bromide functionality to grow diblock, PS-*b*-MMA grafts from the MWNTs. The MWNTs-*g*-polymers (PMMA and PS) showed a large increase in the glass transition temperature ( $T_g$ ) for the grafted chains ( $15 < \Delta T_g < 30$  °C). It is not clear whether the increase in  $T_g$  of the polymer brushes (attached to the MWNTs) is related to a substantial reduction of polymer chain-dynamics or to non-covalent interactions of polymer chains with the  $\text{sp}^2$  network of MWNTs.

Kinetic studies of the SIP of S and MMA showed the evidence of premature termination after  $\sim 8$  h. The plot of wt% of PMMA on the MWNTs with time indicated that the growth of

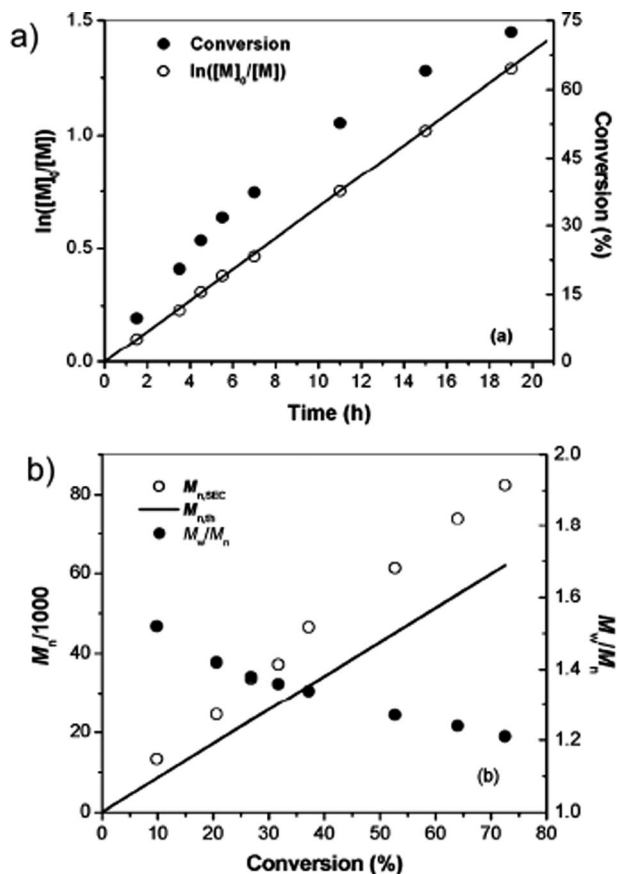


**Fig. 1** Surface initiated ATRP of *n*-BMA from SWNTs. (a) First-order time-conversion plot and (b) dependence of  $M_n$  and  $M_w/M_n$  on conversion in the presence of sacrificial initiator, in DCB at 60 °C. Conditions: [*n*BMA]:[SWNT-initiator + initiator] (1 : 20); [CuCl]:[Biby] = 600 : 1 : 1 : 2. Reprinted with permission from *J. Am. Chem. Soc.*, 2004, **126**, 170.

the polymerization was very slow and reached a maximum after 10 h with low monomer conversion (Fig. 2b). They also observed that a small portion of the MWNTs-*g*-polymers that are soluble in  $\text{CHCl}_3$  at room temperature contain presumably shorter carbon nanotubes with higher wt% of grafted polymers. A small portion of dissolved polymer was separated while recovering the polymer grafted tubes *via* filtration. After evaporation of the solvent, the filtrate had a polymer that appeared slightly grayish in color. This indicated that the recovered fraction in the filtrate contains a large amount of polymer grafted to small amount of MWNTs (0.1–0.2 wt% by TGA). Analysis by SEC showed very large molecular weight species with broad distribution ( $1.4 < M_w/M_n < 3.0$ ) due to the presence of the grafted tubes. In the case of PS grafting, the PS present in the recovered MWNTs-*g*-PS was cleaved from the MWNTs through basic hydrolysis of ester linkage and analyzed by SEC. The analysis showed the presence of PS having molecular weights lower than  $2000 \text{ g mol}^{-1}$  with polydispersity indices between 1.1 and 1.34. This is in accordance with the results obtained by Gao *et al.*<sup>26</sup> who showed the cleaved PS from the MWNTs exhibited a broad polydispersity ( $M_w/M_n \sim 3$ ). The very low concentration of the initiator and the reaction of growing

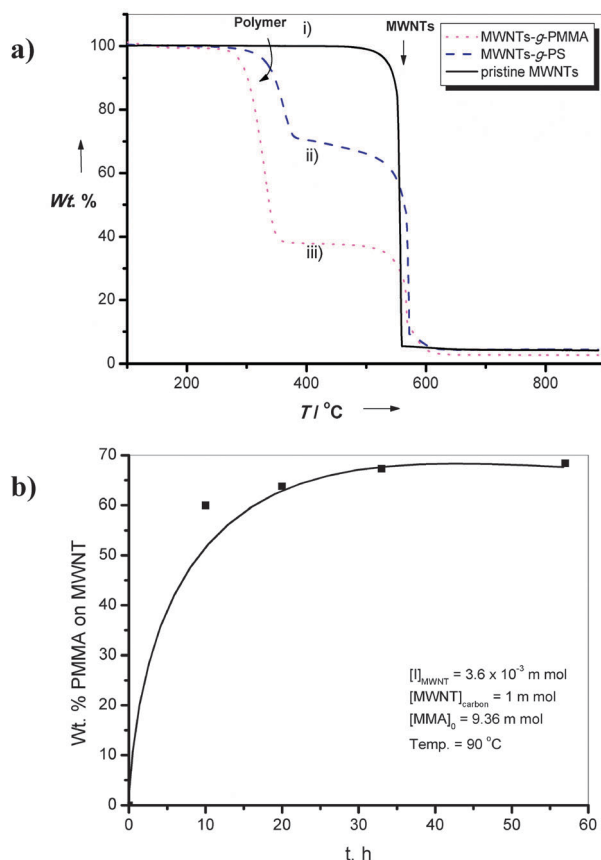


**Fig. 2** Surface initiated ATRP from MWNTs. (a) TGA of MWNTs-*g*-PMMA and MWNTs-*g*-PS in comparison with pristine MWNTs, and (b) weight percent of PMMA grown from MWNTs during the surface initiated ATRP. Reprinted with permission from *Angew. Chem. Int. Ed.*, 2004, **43**, 2138.

radicals with  $\text{sp}^2$  carbons of MWNTs were attributed to the uncontrolled polymerization *via* ATRP.

A majority of the reports on SIP from CNTs deals with the grafting of PS and PMMA (Table 1).<sup>19,27</sup> The MWNTs were grafted with PMMA and PS using a two-step “diazonium salt/ATRP” process, as described by Matrab *et al.*<sup>28</sup> The MWNTs were first modified by electrochemical reduction of brominated aryl diazonium salts (12) and were later used for the surface initiated ATRP of S and MMA. The dependence of the diameter and the length of the MWNTs on the efficiency of the SIP of S was examined by Abetz *et al.*<sup>29</sup> An ATRP initiator was anchored on the surface through three glycol spacers such as diethylene glycol, and poly(ethylene glycol)s (PEG)s with molecular weights 200 and  $400 \text{ g mol}^{-1}$ . The dimensions of the MWNTs, the  $M_n$  of the glycol spacer, and the weight ratio of the monomer to the grafted initiator are the variables that appeared to influence the grafting efficiency. They reported that the highly aggregated shorter MWNTs produced a higher percentage of polystyrene grafted onto the tubes when compared to longer and less aggregated tubes. However, a high wt% of PS can be grafted even from lengthy MWNTs when a right combination of PEG spacer, concentration of the anchored initiator, and monomer/MWNTs weight ratio was employed in the reaction.

**Table 1** Vinyl polymerization (ATRP, RAFT, NMRP, Anionic)

Type of CNTs	Initiator functionality	Monomer <sup>a</sup>	Catalyst/ligand <sup>b</sup>	Solvent <sup>c</sup> / temperature/time	[I] <sub>0</sub> <sup>d</sup> (×10 <sup>5</sup> mol)	[M] <sub>0</sub> mol L <sup>-1</sup>	wt% Grafted <sup>e</sup> polymer	Ref.
Polymerization: ATRP								
SWNTs	(4)	MMA	CuBr/bpy	DMF + H <sub>2</sub> O/RT/24 h	—	2.56	—	16
		<i>t</i> -BA	CuBr/bpy	DMF + H <sub>2</sub> O/RT/24 h	—	1.88	—	20
MWNTs	(1)	MMA	CuBr/PMDETA	DMF/60 °C/30 h	2.11	1.02,	82	22
		MMA + HEMA	CuBr/PMDETA	DMF/60 °C/20 h	—	0.78	54.5	
MWNTs	(2)	MMA	CuBr/PMDETA	Bulk/90 °C/24 h	4.6	—	59–71	19
		S	CuBr/PMDETA	Bulk/100 °C/24 h	19.2	—	18–33	
		MMA + S	CuBr/PMDETA	Bulk/100 °C/24 h	9.6	—	24.6	
SWNTs	(3)	<i>n</i> -BMA	CuCl/bpy	DCB/60 °C/19 h	0.48	12.6	69	55
	(1)				1.93	0.96		54
MWNTs	(1)	S	CuBr/PMDETA	Diphenyl ether/100 °C/ 50 h	1.05	0.96	78	32
					0.72	1.44		54
SWNTs	(3)	S	CuBr/bpy	DCB/110 °C/14 h	0.50	13.12	75	58
MWNTs	(1)	NIPAAAM	CuBr/PMDETA	H <sub>2</sub> O/RT/48 h	2.11	2.20	84	18
MWNTs	(1)	S + <i>t</i> -BA	CuBr/PMDETA	Diphenyl ether/100 °C/ 50 h, DMF/60 °C/48 h	9.9	2.88	70	17
				Methanol/40 °C/48 h	12.0	1.66	90	57
								26
MWNTs	(2)	BBEA	CuBr/PMDETA	Toluene/100 °C/24 h	4.2	—	80	61
MWNTs	(1)	S	CuBr/PMDETA	DMF/130 °C/30 h	2.1	0.24	68	44
SWNTs	(7)	S	CuCl/PMDETA	Ac/60 °C/96 h	—	87.4	—	27
SWNTs	(5)	MPC	CuBr/bpy	H <sub>2</sub> O/RT/ 12 or 24 h	0.56	0.34	59	34
		LAMA	CuBr/bpy	H <sub>2</sub> O/RT/12 h	0.37	0.2	67	
		LAMA	CuBr/bpy	NMP/RT/12 h	0.37	0.2	70	
MWNTs	(1)	DEAEMA	CuBr/PMDETA	Methanol/60 °C/48 h	9.9	1.35	67	43
MWNTs	(12)	S	CuBr/PMDETA	Bulk/110 °C/16 h	—	—	—	28
		MMA	CuCl + CuCl <sub>2</sub> / PMDETA	Bulk/90 °C/6 h	—	—	—	
MWNTs	(13)	S	CuBr/dNbpy	Toluene/110 °C/18 h	12.8	8.74	40	38
								39
MWNTs	(1)	DMAEMA	CuBr/PMDETA	THF/60 °C/48 h	7.14	3.18	80	42
MWNTs	(1)	S	CuBr/PMDETA	Anisole/90 °C/20 h	24.0	—	85	29
MWNTs	(11)	S	CuBr/PMDETA	Bulk/110 °C/18 h	—	—	4–47	51
MWNTs	(1)	MAIG	CuBr/HMTETA	Ethyl acetate/60 °C/29 h	4.2	1.69	71	62
		BIEMA	CuBr/(PPh <sub>3</sub> ) <sub>2</sub> NiBr <sub>2</sub>	Ethyl acetate/100 °C/4.5 h	—	1.9	38	
		MAIG + BIEMA	CuBr/(PPh <sub>3</sub> ) <sub>2</sub> NiBr <sub>2</sub>	Ethyl acetate/100 °C/ 4.5–29.5 h	—	—	40–53	
MWNTs	(2)	S	CuBr/PMDETA	Bulk/80 °C/24 h	1.6	—	60	45
		An	CuBr/PMDETA	Bulk/70 °C/24 h	1.6	—	40	
		S + An	CuBr/PMDETA	Bulk/80 °C/24 h	1.6	—	70	
SWNTs	(19)	MMA	CuBr/PMDETA	DCB/60 °C/24 h	0.26	6.0	30	30
								31
MWNTs	(10)	S + NIPAM	CuBr/PMDETA	Diphenyl ether/80 °C/50 h, H <sub>2</sub> O/RT/48 h	13.0	1.6	42	59
MWNTs	(1)	<i>n</i> -BMA	CuBr/bpy	Bulk/70 °C/72 h	5.88	—	23	48
SWNTs	(16,17)	Vq	CuBr/PMDETA	DMF/110 °C/18 h	1.1	0.024	59	49
MWNTs	(1)	BIM-PF <sub>6</sub>	CuBr + CuBr <sub>2</sub> / PMDETA	Propionitrile/90 °C/ 8–32 h	1.7	0.68	20–51	37
MWNTs	(14)	S	CuBr/PMDETA	Bulk/80 °C/24 h	2.8	—	33	96
		MMA	CuBr/PMDETA	THF/40 °C/24 h	2.8	2.5	51	
		GMA-N <sub>3</sub>	CuBr/PMDETA	THF/RT/24 h	1.7	1.46	58	
MWNTs	(6)	GMA	CuBr/bpy	Ethanol + H <sub>2</sub> O/RT/24 h	0.89	0.28	65	47
SWNTs	(9)	<i>n</i> -BA	CuBr/PMDETA	Diphenyl ether/80 °C/ 7–18.5 h	2.0	88.2	—	46
MWNTs	(2)	TMSPMA	CuBr/PMDETA	DMAC/60 °C/30 h	7.6	0.6	56–93	52
MWNTs	(8)	S	CuBr/HMTETA	Bulk/120 °C/19 h	0.6	—	76	60
		MMA	“	“	“	“	“	
MWNTs	(2)	MMAZO	CuBr/HMTETA	Chloro benzene/85 °C/48 h	0.8	0.63	52–67	50
MWNTs	(2)	S	CuBr <sub>2</sub> /Me <sub>6</sub> TREN/ Sn(EH) <sub>2</sub>	Anisole/100 °C/—	—	17.4	9–85	53
MWNTs	(1)	MPC	CuBr + CuBr <sub>2</sub> /bpy	Ethanol + H <sub>2</sub> O/RT/24 h	1.3	0.3	48	35
MWNTs	(15)	SPM	CuCl <sub>2</sub> /bpy	DMF + H <sub>2</sub> O/40 °C /24 h	—	0.7	—	56
								36
MWNTs	(18)	S	CuBr + CuBr <sub>2</sub> /PMDETA	Bulk/90 °C/24 h	—	—	48	40
SWNTs	(20)	S	—	—	—	—	—	41
Polymerization: RAFT								
MWNTs	(21)	S	AIBN	THF/100 °C/24 h	1.02	0.19	32–62	66

Table 1 (continued)

Type of CNTs	Initiator functionality	Monomer <sup>a</sup>	Catalyst/ligand <sup>b</sup>	Solvent <sup>c</sup> / temperature/time	[ <i>I</i> ] <sub>0</sub> <sup>d</sup> (×10 <sup>5</sup> mol)	[ <i>M</i> ] <sub>0</sub> mol L <sup>-1</sup>	wt% Grafted <sup>e</sup> polymer	Ref.
MWNTs	(21)	NIPAM	AIBN	Benzene/100 °C/ 9–36 h	2.73	4.42	35–87	68
MWNTs	(21)	HPMA	AIBN	Methanol/60 °C/8–28 h	3.85	1.74	35–77	74
MWNTs	(21)	S + Mah	AIBN	THF/80 °C/–	—	1.2	42	67
MWNTs	(21)	NIPAM	AIBN	Benzene/90 °C/16 h	0.96	0.88	23–85	69
MWNTs	(21)	MMA + S	AIBN	THF/90 °C/48 h, DMF/90 °C/24 h	1.92	0.8	76	72
MWNTs	(21)	MDMAS DMAEMA AA	AIBN	Solvent/60 °C/20 h Solvent/60 °C/15 h Solvent/60 °C/15 h	— — —	0.95 1.59 3.47	78 69 50	73
MWNTs	(21)	S S + NIPAM	AIBN	Benzene/90 °C/24 h Benzene/90 °C/10–30 h	1.92	1.44	37 56–86	70
MWNTs	(21)	MMA	AIBN	THF/90 °C/20 h	0.77	0.4	22–67	71
MWNTs	(22)	HEMA	AIBN	DMF/70 °C/8–32 h	0.97	2.42	26–78	75
MWNTs	(23)	S	AIBN	DMF/100 °C/8–24 h	1.25	2.4	20–69	76
SWNTs	(24)	Am	AIBN	Benzene/60 °C/12–50 h	4.47	2.81	46–78	77
MWNTs	(25)	VC	AIBN	THF/70 °C/24 h	1.6	0.2	58–96	78
Polymerization: NMRP								
<i>N</i> -MWNTs	(26)	S	BPO	Solvent/130 °C/24 h	—	—	35	80
MWNTs	(27)	4VP 4SS	TEMPO TEMPO	DMF/125 °C/24 h DMF/125 °C/24 h	0.46	2.25	30 30	81
MWNTs	(27)	S S + 4VP	TEMPO TEMPO	Chlorobenzene/125 °C/ 24–48 h DMF/125 °C/48 h	0.46	15.86	12–61 67	82
MWNTs	(28)	S	TEMPO	Bulk/120 °C/24 h	2.82	—	30	83
MWNTs	(29)	S	TEMPO–OH	Bulk/130 °C/4 h	1.71	—	20	84
Polymerization: Anionic								
SWNTs	(30)	S	—	Cyclohexane/48 °C/2 h	—	—	10	86
SWNTs	(30)	<i>t</i> -BA <i>t</i> -BA + MMA	—	THF/–78 °C/3 h THF/–78 °C/6 h	6.14	0.51	29 47	87
SWNTs	(31)	MMA	—	NH <sub>3</sub> /RT/Overnight	—	—	45	88
MWNTs	(32)	S S + I	—	Benzene/RT/0.75–1.5 h Benzene/RT/42 h	3.93	0.86	86–98 99	89

<sup>a</sup> S: Styrene, MMA: Methyl Methacrylate, *t*-BA: *tert*-Butyl Acrylate, *n*-BMA: *normal*-Butyl Methacrylate, DMAEMA: Dimethylaminoethyl Methacrylate, DEAEMA: Diethylaminoethyl Methacrylate, An: Acrylonitrile, AA: Acrylic Acid, HEMA: Hydroxyethyl Methacrylate, HPMA: Hydroxypropylmethyl Methacrylamide, NIPAM: *N*-Isopropyl Acrylamide, GMA: Glycerol Methacrylate, BBEA: 2-((Bromobutyl)oxy) ethyl Acrylate, MPC: 2-Methacryloyloxyethyl Phosphorylcholine, LAMA: Lactobion Amidoethylmethacrylate, MAIG: 3-*O*-Methacryloyl-1,2:5,6-di-*O*-Isopropylidene- $\beta$ -Glucopyranose, BIEMA: 2-(2-Bromoisobutyryloxy)ethyl Methacrylate, Vq: Vinylquinoline, 4-VP: 4-Vinyl Pyridine, TMSPPMA: 3-(Trimethoxysilyl)propyl Methacrylate, MMAZO: 6-[4-(4-Methoxyphenylazo)-phenoxy]hexyl Methacrylate, SPM: 3-Sulfopropylamino Methacrylate, MAH: Maleic Anhydride, MDMAS: 3-[*N*-(3-Methacrylamidinopropyl)-*N,N*-Dimethyl] Ammonio propane Sulfonate, BIM-PF<sub>6</sub>: 2-(1-Butylimidazolium-3-yl)ethyl Methacrylate Hexafluorophosphate, Am: Acrylamide, VC: Vinyl Carbazole, 4-SS: 4-Styrene Sulfonate, and I: Isoprene. <sup>b</sup> PMDETA: *N,N,N',N''*-Pentamethyldiethylenetriamine, HMTETA: 1,1,4,7,10,10-Hexamethyltriethylenetetramine, bpy: 2,2'-bipyridine, dNbpy: 4,4'-dinonyl-2,2'-bipyridine, AIBN: Azobisisobutyronitrile, TEMPO: (2,2,6,6-Tetramethylpiperidin-1-yl)oxyl, BPO: Benzoyl Peroxide. <sup>c</sup> DMF: Dimethyl formamide, Ac: Acetone, THF: Tetrahydrofuran, DCB: Dichloro Benzene, NMP: *N*-Methyl Pyrrolidone, and DMAc: *N,N*-dimethylacetamide. <sup>d</sup> Moles of initiator present on the total grams of CNTs in the reaction. <sup>e</sup> Determined by TGA with respect to carbon. (—) Data not available.

A different approach to the surface modification of SWNTs with a direct radical addition of peroxy organic acids, such as *m*-chloroperbenzoic and 2-bromo-2-methylperpropionic (**19**) acids under ultrasonication, was demonstrated by Liu *et al.*<sup>30</sup> The functional groups, resulting from the decomposition of peroxy organic acids, were used as a source for the covalent introduction of the ATRP initiator moiety onto the SWNTs. Surface initiated ATRP of MMA was examined from the initiator functionalized SWNTs and the authors observed that, when the sacrificial initiator was introduced into the polymerization medium, the grafted PMMA content on the SWNTs increased to 30 wt%. On the other hand, only 17 wt% polymer content was achieved using the grafted initiator. Furthermore, when MMA and catalyst/ligand were introduced into the solution in the presence of unfunctionalized SWNTs, around 8 wt% of PMMA was covalently grafted onto the CNTs. This indicated that the nanotubes acted as radical scavenger and the growing

polymer radicals initiated by heat could react with the nanotubes. The same group have also used halogen containing organic solvents, such as *o*-dichlorobenzene (ODCB) and polymerized MMA *in situ* using CuBr/Ligand by ultrasonication.<sup>31</sup> It was proposed that ODCB was decomposed during sonication and generated radicals that reacted with the sidewalls of the CNTs. However, the purpose of ATRP catalyst in the system was not clearly defined as the system did not have any potential alkylhalide initiator for the polymerization of MMA *via* ATRP.

Gao *et al.*<sup>32</sup> described grafting of *N*-isopropylacrylamide (NIPAM) from MWNTs using surface initiated ATRP to generate temperature-sensitive poly(*N*-isopropylacrylamide) (PNIPAM). The polymerization process was not controllable as evident from the low molecular weight of the grafts and the high polydispersity indices of the grafted samples. High resolution transmission electron micrograph (HRTEM) images clearly showed the difference between pristine MWNTs, Fig. 3 (a),



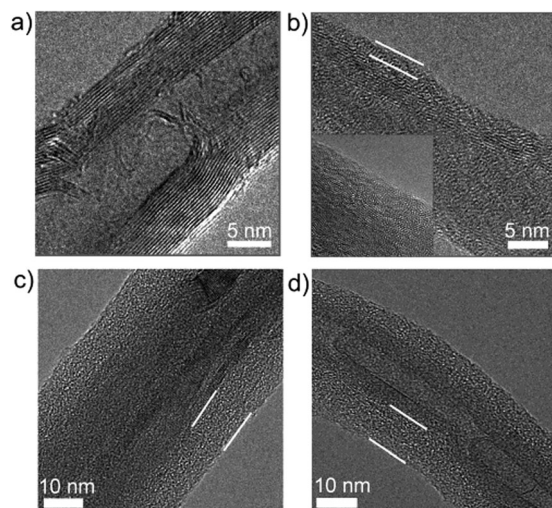


**Fig. 3** HRTEM images of crude MWNT (a), NTP1 (b), NTP2 (c), and NTP3 (d). Inset of image b: local amplification of NTP1. The marked polymer shells in images b–d have thicknesses of 3, 11, and 14 nm, respectively. Reprinted with permission from *Macromolecules*, 2004, **37**, 6683.

and the polymer functionalized MWNTs, Fig. 3 (b), (c) and (d). Core-shell structures were observed with the polymer layer thickness ranging from 3 to 14 nm. The synthesized MWNTs-*g*-PNIPAM showed temperature-sensitive collapse in water (at 30–35 °C), due to lower critical solution temperature (LCST) behavior of PNIPAM.

Similarly, Sun *et al.*<sup>33</sup> reported the functionalization of aligned carbon nanotubes (ACNTs) with PNIPAM through the surface initiated ATRP. Macroscopically the ACNT films showed reproducible temperature-sensitive wettability, while microscopically the individual CNTs on the films were also temperature responsive since, their diameter changed with temperature, as noticed *via* AFM studies.

Different types of vinyl polymers have been subsequently grafted from CNTs by various groups using ATRP. Very important polymers based on cyclic carbohydrates and phosphorylcholine, that find applications in carbohydrate-protein recognition and in cell membrane, have been grafted from SWNTs by Narain *et al.*<sup>34</sup> SWNTs were functionalized with bromoisobutyrate and were used for the surface initiated ATRP of 2-methacryloyloxyethyl phosphorylcholine (MPC), and lactobion-amidoethylmethacrylate (LAMA). The characterization of polymer grafted SWNTs by TGA, Raman, and <sup>1</sup>H-NMR confirmed the presence of sugar repeat units of LAMA (Fig. 4). Two different catalyst/ligand systems were used for the SIP of LAMA in NMP. Well-defined brushes were obtained when using a CuCl/bpy catalyst system. The initiator efficiency was low, and the polydispersity indices were below 1.25, as monitored by SEC, after the cleavage of the polymer chains. The polydispersity indices were higher than 1.7 and 2.1 in NMP and water, respectively, when CuBr was used as a catalyst. Both SWNTs-*g*-PMPC and SWNTs-*g*-PLAMA were found to be soluble in water, while the former was soluble also in MeOH and the latter in NMP. Zhu *et al.*<sup>35</sup> reported grafting of MPC with MWNTs and extended their study on the effects of MWNTs-*g*-PMPC on blood coagulation.

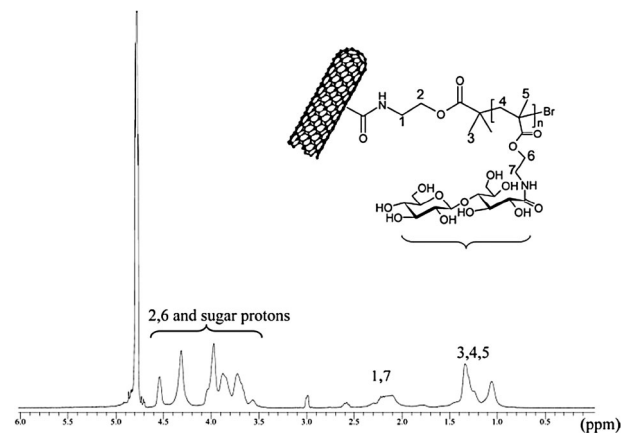


**Fig. 4** <sup>1</sup>H-NMR of poly(lactobion amidoethylmethacrylate) (PLAMA) grafted SWNTs (SWNTs-*g*-PLAMA) synthesized using surface initiated ATRP. Reprinted with permission from *J. Polym. Sci. Part A: Polym. Chem.*, 2006, **44**, 6558.

Recently, Romero *et al.*<sup>36</sup> functionalized MWNTs with polyelectrolyte brushes and lipid layers to control their intercellular distribution and *in vitro* toxicity. It was revealed that the polyelectrolyte coated MWNTs had higher toxicity than lipid coated MWNTs.

A core-shell structure was formed when 2-bromoisobutryl bromide modified MWNTs were used to graft an ionic-liquid containing monomer, 2-(1-butylimidazolium-3-yl)ethyl methacrylate hexafluorophosphate (BIM-PF<sub>6</sub>).<sup>37</sup> The TGA of the polymer grafted MWNTs indicated that the amount of grafted poly(ionic liquid) (PIL) was increased with polymerization time achieving a maximum of 50 wt% PIL in MWNTs-*g*-PIL. The effect of various counter anions on the solubility of the MWNT-*g*-PILs was investigated revealing that the relative solubility in water and organic solvents could be switched by anion exchange, constructing a reversible phase-transition cycles. It was also shown that MWNT-*g*-PILs, due to their good dispersibility in lubricants, can be used as additives to improve the anti-wear and friction reducing properties of lubricants. Nitrogen doped-MWNTs, CN<sub>x</sub>MWNTs, were first used by Fragneaud *et al.*<sup>38</sup> as a substrate for surface initiated ATRP. Free radicals were used to graft brominated aromatic rings on the CN<sub>x</sub>MWNTs, which served as initiating sites for the ATRP of styrene (13). The CN<sub>x</sub>MWNTs were homogeneously covered by an amorphous layer of PS up to 3–5 nm thickness, as revealed by HRTEM images. The same authors have also used CN<sub>x</sub>MWNTs-*g*-PS in conjunction with PS and poly(butadiene-*co*-styrene) to synthesize nanocomposites.<sup>39</sup>

Abetz and co-workers<sup>40</sup> studied the Diels-Alder cycloaddition of furfuryl-2-bromoisobutyrate (diene) and other dienophile molecules toward SWNTs and MWNTs and found that CNTs behave dually either as diene or dienophile depending on the type of reactants used in the reaction. Using an ATRP initiator functionalized furfuryl adduct of MWNTs, they polymerized S and grafted PS up to 48 wt%. Another Diels-Alder cycloaddition reaction was very recently performed for the covalent functionalization of SWNTs. The selectivity of the reaction towards metallic and semiconducting SWNTs was examined.<sup>41</sup> In this study, 1-aminoanthracene was used as the electron rich diene molecule in a reaction that took place in diethylene glycol under high temperature for 24 hours (20). The product (20) was washed

many times to remove the physically adsorbed substituted anthracene through  $\pi$ - $\pi$  interactions. The degree of functionalization was controlled by the temperature of the reaction. The *s*-SWNTs with the larger diameter exhibited a higher reactivity compared to the *m*-SWNTs. The amine substituted SWNTs were further functionalized with 2-bromo-2-methylpropionyl bromide and S was grafted *via* ATRP.

Other polymers that have been grafted onto MWNTs and SWNTs are poly(dimethylaminoethyl methacrylate) (PDMAEMA),<sup>42</sup> poly(diethylaminoethyl methacrylate) (PDEAEMA),<sup>43</sup> poly(*tert*-butyl acrylate), poly(styrene-*b*-acrylic acid) (PAA),<sup>44</sup> poly(sodium 4-styrenesulfonate) (PSS),<sup>42</sup> poly(styrene-*co*-acrylonitrile),<sup>45</sup> poly(*n*-butyl acrylate) (PnBA),<sup>46</sup> poly(glycidyl methacrylate),<sup>47</sup> and poly(*n*-butyl methacrylate) (Table 1).<sup>48</sup> In all the above cases, the growth of the polymer from the CNTs was not homogeneous.<sup>19,46</sup> The grafting density was found to vary widely, depending on the monomer and the polymerization conditions. In the case of ATRP of *n*BA from SWNTs, the density varied from  $\sim 1.0$ – $10.0$  chains  $\text{nm}^{-1}$ , assuming that the grafted polymer chains were fully extended, indicating chemical heterogeneity along and in between the individual SWNTs. The mid-section of the tubes appeared to have a high grafting density.<sup>46</sup> The variation of the grafting density was ascribed to a non-uniform initiator functionalization along the nanotubes and to the van der Waals induced aggregation of the CNTs.

Polymer grafted CNTs have been used as a compatibilizer for blending CNTs with other polymers. Shi *et al.*<sup>48</sup> used MWNTs-*g*-PnBMA to prepare nanocomposites of poly(vinyl chloride) with as low as 0.1 wt% MWNTs content that showed a significant improvement in mechanical properties. A photoactive vinyl quinoline was polymerized from the SWNTs functionalized with an ATRP initiator. Photoluminescence studies indicated that the quinolone units of the covalently attached polymer greatly influence the optical property. The studies further showed an electron transfer from excited quinoline units into the SWNTs. Although up to 60 wt% of the polymer was grown from the surface, it accounted for only 7–8 monomer repeat units per initiating site.<sup>49</sup>

The preparation and the orientation behavior of MWNTs grafted with a side-chain azobenzene liquid crystalline poly(6-[4-(4-methoxyphenylazo)phenoxy]hexyl methacrylate) (PMMAZO),

*via* ATRP, were recently reported by Hu *et al.*<sup>50</sup> Differential scanning calorimetry (DSC) and polarized optical microscopy showed that the liquid crystalline behavior of MWNT-*g*-PMMAZO and a neat PMMAZO was similar. The orientation of MWNTs in a PMMAZO matrix, under the influence of an electric field, was dominated by the viscosity of the matrix. On the other hand, the orientation of MWNTs-*g*-PMMAZO was controlled by both the viscosity and the liquid crystalline phase due to a better compatibility between MWNTs and PMMAZO after the covalent modification.

The importance of the MWNTs starting material in the reactivity and the polymer loading was underlined in another study.<sup>51</sup> A UV sensitive ATRP-initiator was attached directly to pristine MWNTs (**11**) by exposure to UV light, and a series of S polymerizations were conducted. Scanning electron micrographs of the two different pristine MWNTs (Fig. 5) and the PS functionalized ones (Fig. 6) showed that tubes with the low aspect ratio were almost the same, due to the low PS loading (Fig. 6A and 7A). Furthermore, tubes with high aspect ratio showed a matrix of PS enveloping the CNTs (Fig. 7B). Surface initiated ATRP of S was optimized using pentamethyldiethylenetriamine (PMDETA) as a ligand. The MWNTs with a high aspect ratio were used for the study. SEC analysis after cleaving the PS showed a number average molecular weight of  $40\,000\text{ g mol}^{-1}$  and a polydispersity of 1.5 for MWNTs grafted with 47 wt% PS.

ATRP was also employed for the polymerization of 3-(trimethoxysilyl)propyl methacrylate from the initiator grafted MWNTs.<sup>52</sup> TGA indicated that the amount of polymer on the tubes can be controlled by the monomer to initiator mole feed ratio. After hydrolysis of the grafted polymer, a highly cross-linked polymeric network was formed *via* intermolecular condensation around the CNTs. The polymeric network coated CNTs were insoluble in organic solvents.

Aitchison *et al.*<sup>53</sup> reported the use of Activators Regenerated Electron Transfer (ARGET) ATRP for the functionalization of MWNTs with PS brushes. They obtained MWNTs-*g*-PS with up to 84.7 wt% of PS. The PS grafted onto the MWNTs exhibited a high glass transition temperature ( $\Delta T_g \sim 14.0\text{ }^\circ\text{C}$ ). A low catalyst concentration and a limited air tolerability of the ARGET process make this technique more viable for scale up operation.

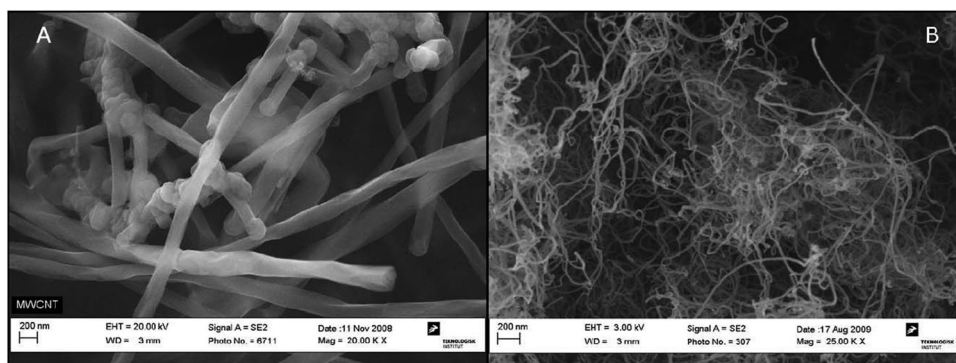


**Fig. 5** Scanning electron micrographs of two different grades of pristine MWCNT. (A) pristine MWNTs from Sigma-Aldrich, and (B) pristine MWNTs from Nanocyl (B). Reprinted with permission from *J. Polym. Sci. Part A: Polym. Chem.*, 2010, **48**, 4594.

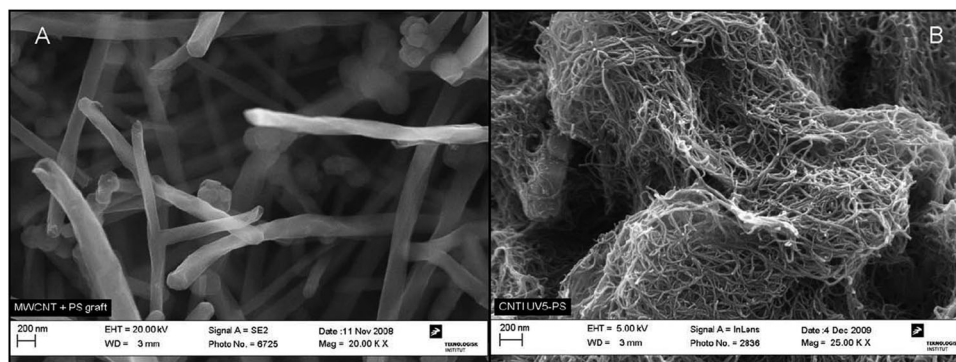


**Fig. 6** Scanning electron micrographs of polystyrene-grafted MWNTs, (A) Sigma-Aldrich MWNTs-g-PS and (B) Nanocyl MWNTs-g-PS. Reprinted with permission from *J. Polym. Sci. Part A: Polym. Chem.*, 2010, **48**, 4594.

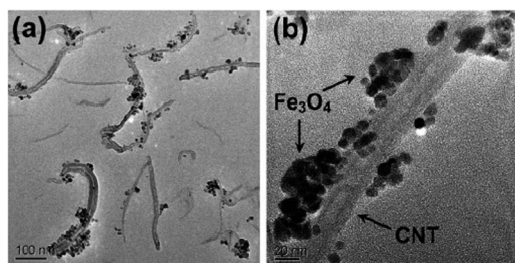


**Fig. 7** TEM images of the MWNT-g-PAmI deposited with magnetic  $\text{Fe}_3\text{O}_4$  nanoparticles. Reprinted with permission from *J. Phys. Chem. B*, 2006, **110**, 7213.

The polymer layer thickness around the CNTs, as revealed by TEM and TGA, increased with polymerization time. The molecular weight of the chains, cleaved from the surface after 50 h of the polymerization, was close to  $95\,000\text{ g mol}^{-1}$  with a polydispersity index of 1.8. The MWNTs-g-PS were used as fillers in a PS matrix, where a uniform dispersion of the filler was observed for concentrations up to 1.0 wt%. The transparency of the nanocomposite film decreased with increasing concentration of MWNTs-g-PS and for concentrations above 0.25 wt% the product was completely opaque.

A layer-by-layer approach was used to prepare self-assembled nanowires using MWNTs-g-PSS as polyanion and MWNTs-g-PDMAEMA as polycation.<sup>42</sup> The starting template was MWNTs-COOH, which showed a high efficiency for loading polyelectrolytes since the polymer quantity adsorbed was more than 10 wt% in every deposition step. High resolution TEM was utilized for the evaluation of the morphology of nanowires. Core-shell morphology was observed with a tubular structure of the MWNT core and the outer shell containing a smooth and flat polymer layer of uniform thickness. A strange self-assembly behavior of MWNTs-g-PMMA (80 wt%) in THF was reported that it formed structures like basketworks, cellular networks and needles.<sup>54</sup> Authors attributed the formation of these self-assembled structures to the polymer phase separation and aggregation during the evaporation of THF.

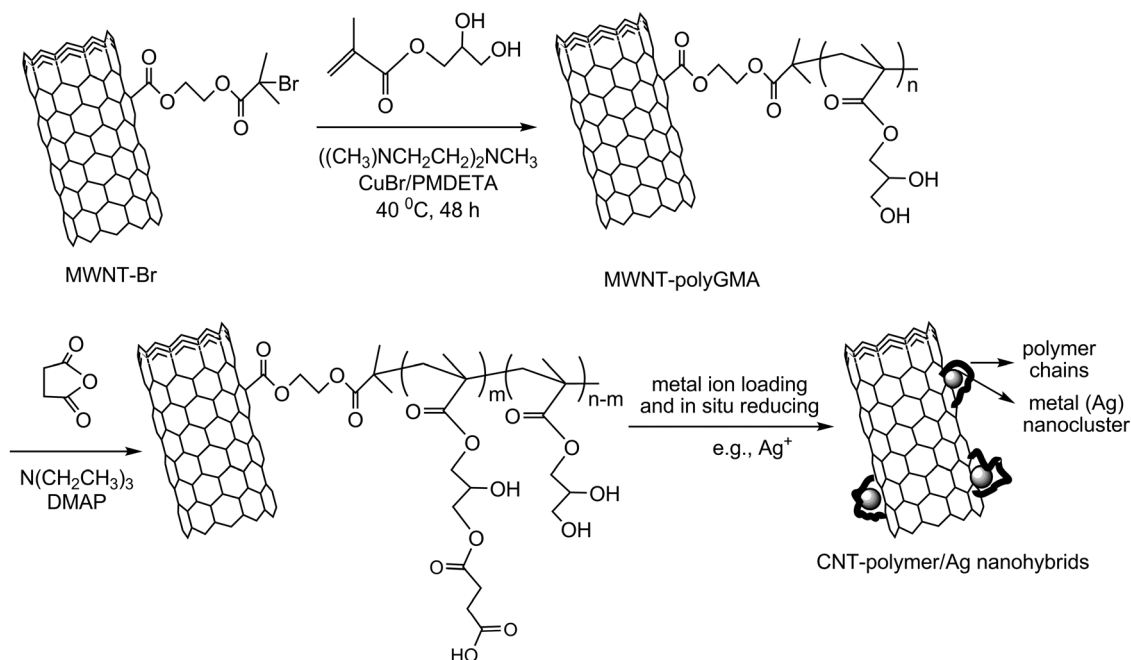
**2.1.1.1 Nanoparticles self-assembly on CNTs-g-polymer.** Grafting of polymers from the CNTs using ATRP has been proven extremely helpful for the attachment of various semi-conducting and

magneto-nanoparticles on the walls of CNTs. Reaction of methyl iodide with MWNTs-g-PDMAEMA has been used to form cationic polyamine coated MWNTs (MWNTs-g-PAmMeI).<sup>55</sup> Cationic polyamine grafted MWNTs and amine functionalized MWNTs (MWNTs-NH<sub>2</sub>) have been used for the assembly of CdTe quantum dots (QDs) as well as  $\text{Fe}_3\text{O}_4$  magnetic nanoparticles on the surface of MWNTs through interactions with amino- and ammonium salt of the grafted polymer. The optical property of CdTe QDs and the magnetic properties of  $\text{Fe}_3\text{O}_4$  nanoparticles were maintained in the resulting hybrids when MWNT-PAmMeI was used. In contrast, the photoluminescence spectrum of the MWNTs-NH<sub>2</sub>/CdTe composite showed no emission peak, which was probably due to the direct addition of the CdTe (QDs) on the MWNTs surface. It was suggested that the electrons from the electron-hole pairs were directly flowing into the CNTs quenching the photoluminescence of CdTe crystals. In a different approach, poly(3-sulfopropylamino methacrylate) brushes grafted MWNTs were utilized as a substrate for the immobilization of CdS nanocrystals or  $\text{Fe}_3\text{O}_4$  magnetic nanoparticles, through ion exchange with the cations of the sulfonate groups. The CNTs-organic-inorganic hybrids were well characterized by TEM.<sup>56</sup>

Gao *et al.*<sup>57</sup> functionalized MWNTs with a hydrophilic hydroxylated polymer, poly(glycerol monomethacrylate) PGMA, by surface initiated ATRP. The hydroxyl groups of the grafted polymer were converted into carboxylic acid groups (52–57% yield) by reacting with acid anhydride, resulting in MWNTs with hydroxyl and acid functionalized copolymer grafts that could be aligned by a self-assembly during solvent evaporation. After derivatization, the polyacid functionalized MWNTs were used to sequester metal ions ( $\text{Ag}^+$ ,  $\text{Co}^{+2}$ ,  $\text{Ni}^{+2}$ ,  $\text{Au}^{+3}$ ,  $\text{La}^{+3}$ ,  $\text{Y}^{+3}$ ) forming polymer/metal-MWNTs hybrid materials, nanowires and necklace-like structures, depending on the wt% of the grafted polymer content and the amount of the captured metal (Scheme 4).

In a later work, Gao *et al.*<sup>43</sup> synthesized paramagnetic nanotubes by assembling paramagnetic iron oxide nanoparticles ( $\text{Fe}_3\text{O}_4$ ) onto poly(2-diethylaminoethyl methacrylate) grafted MWNTs. The synthetic process was similar to the one reported earlier by the same group.<sup>57</sup> High resolution TEM revealed a core-shell morphology with a 3–5 nm wrapped polymer layer around the nanotubes. The polyamine grafted





**Scheme 4** Functionalization of MWNTs with PGMA, esterification of the  $-\text{OH}$  groups and metal sequestration/reduction by the grafted polyacid chains.

nanotubes could be used without further modification to immobilize anionic particles by adjusting the pH of the solution. The authors quaternized the MWNT-*g*-(PDEAEMA) with methyl iodide affording cationic polyelectrolyte-grafted MWNTs (MWNT-PAmI), which were loaded with the nanoparticles through an electrostatic self-assembly. The amount of loaded magnetic nanoparticles was controlled by changing the feed ratio of  $\text{Fe}_3\text{O}_4$  to MWNT-*g*-PAmI. The magnetic nanotubes were visualized by HRTEM, different structures were observed depending on the loaded amount of iron oxide nanoparticles (Fig. 7). When the loading was high, the nanoparticles assembled into nanoclusters. At lower loading, the magnetic particles were separated and distributed along the CNTs surface. Also, in areas where there was no polymer grafting, no nanoparticles were observed. The magnetic nanotubes were used as a magnetic-handle to manipulate sheep's red blood cells.<sup>43</sup>

**2.1.1.2 Diblocks and double graft copolymers from CNTs.** The surface initiated ATRP from the CNTs produces polymer grafts with substituted alkylhalide functionality at the chain-ends, which can be

used for re-initiation of other vinyl monomers to produce diblock copolymer grafts. Several diblock copolymers were attached covalently from MWNTs using a two-step method by Baskaran *et al.*<sup>19</sup> and Gao *et al.*<sup>26,42,44</sup> The diblock copolymers grafted from MWNTs include, PS-*b*-PMMA, PMMA-*b*-P(hydroxyethyl methacrylate), PS-*b*-Poly(*t*-butyl acrylate), and PS-*b*-P(acrylic acid).

Recently, Gao *et al.*<sup>58</sup> presented a strategy to grow mixed polymer chains (double grafts) from MWNTs *via* a combination of ATRP and click chemistry using both *grafting from* and *grafting to* methods. A macroinitiator with azido and alkyl bromide functionality was clicked on the alkyne grafted SWNTs and MWNTs. Alkyl bromide functionality was used to initiate ATRP of S and *n*-BMA. The azido functionality was used to click alkyne-terminated PEG, resulting in amphiphilic polymer brushes-grafted MWNTs. The grafted amphiphilic brushes, MWNTs-*g*-(PnBA)<sub>*m*</sub>(PEG)<sub>*n*</sub> and SWNTs-*g*-(PS)<sub>*m*</sub>(PEG)<sub>*n*</sub> were soluble in chloroform and were self-assembled at the interface of a water/chloroform mixture creating *Janus* type structures (Fig. 8).

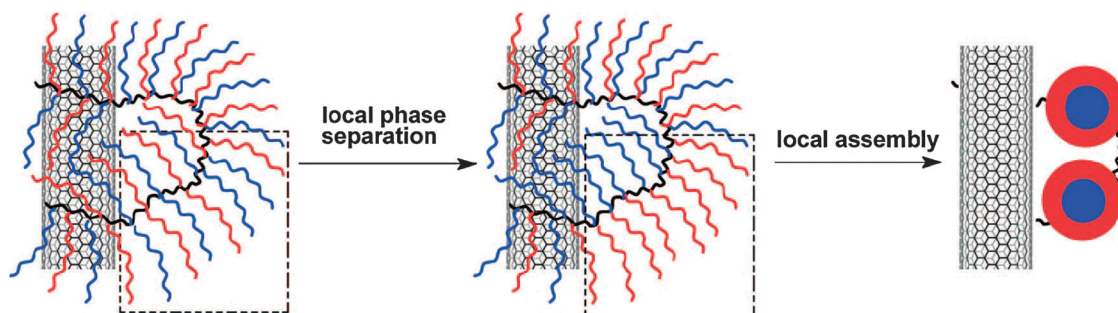
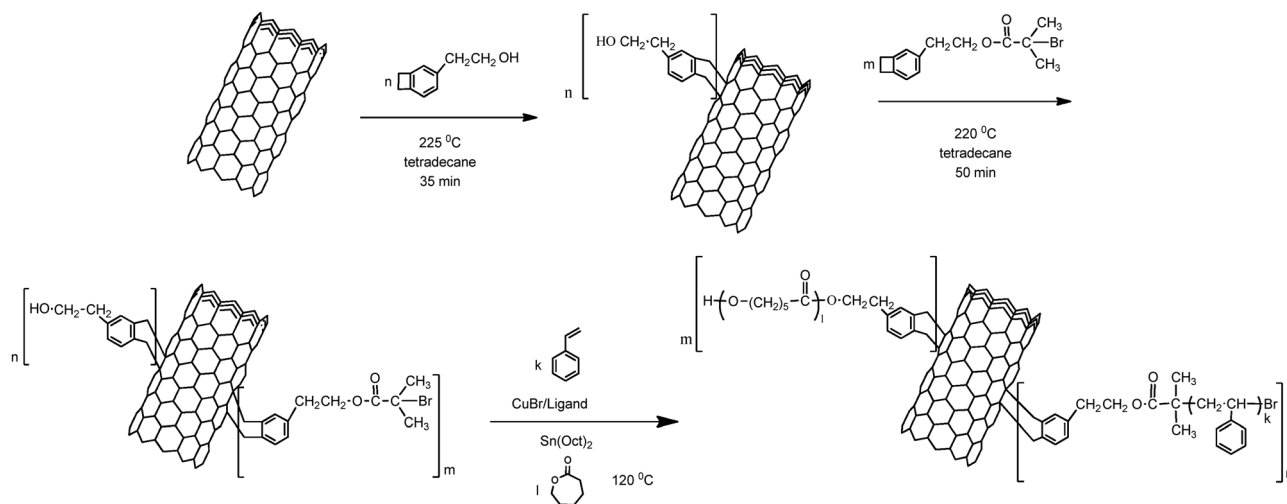


**Fig. 8** Cartoon of the local phase separation and assembly of amphiphilic polymer brushes into *Janus* polymer structures on carbon nanotubes. Reprinted with permission from *Macromolecules*, 2008, **41**, 9581.





**Scheme 5** One-step synthesis of *Janus*-MWNTs grafted with chemically different types of brushes. Notation for a number of functional groups grafted to the different  $sp^2$  carbons on the CNTs is indicated as a group within a bracket with a number "n" for clarity.

Liu *et al.* reported the grafting of a V-shaped PS-*b*-PNIPAAm copolymer (mixed binary polymer chains) and a linear PS-*b*-PNIPAAm copolymer from MWNTs using ATRP.<sup>59</sup> PS-Br was grafted to the MWNTs using the *grafting to* method and the radically transferred bromide on the surface of MWNTs was used as a macro-initiator (**10**) for the synthesis of V-shaped MWNT-*g*-(PS-*b*-PNIPAAm) *via* the *grafting from* method. SIP was employed for the synthesis of linear block copolymers. The necessary initiating sites were formed by the radical addition of 1-bromoethylbenzene onto the CNTs in the presence of CuBr and PMDETA. A similar synthetic route was used for the functionalization of CNTs with PS-Br by the *grafting to* strategy. The tertiary C-Br groups on the tubes were utilized as initiators for the polymerization of NIPAAm to produce the V-shaped brushes. The final nanocomposite materials were soluble in chloroform and when placed in a chloroform/water mixture created a film at the solvent interface. Furthermore, when the temperature was raised to 50 °C the V-shaped diblock grafted MWNTs migrated from the interface to the chloroform phase.

Our group reported<sup>60</sup> a novel one-pot method for the simultaneous growth of two different homopolymers from MWNTs to graft binary polymer brushes. Diels-Alder cycloaddition [4 + 2] reaction was used to functionalize MWNTs with two different precursor initiators, one for ATRP (**8**) and another for ring opening polymerization (ROP). The binary functionalized MWNTs were used for simultaneous SIP of S or MMA through ATRP and  $\epsilon$ -CL or L-LA through ROP (Scheme 5). The rate of ATRP of S was slower than that of the ROP of  $\epsilon$ -CL or L-LA as indicated by the presence of a low mole fraction of PS in the final products, compared to the feed composition. In contrast, the ATRP of MMA was more efficient than that of S. Sequential polymerizations of  $\epsilon$ -CL and S were also conducted under similar experimental conditions in order to verify the non-interference of ROP with ATRP. The MWNTs with multi-grafts of PS and P $\epsilon$ -CL or P $l$ -LA formed *Janus* type structures, when placed in a selective immiscible solvent mixture (cyclohexane/acetonitrile) (Fig. 9).

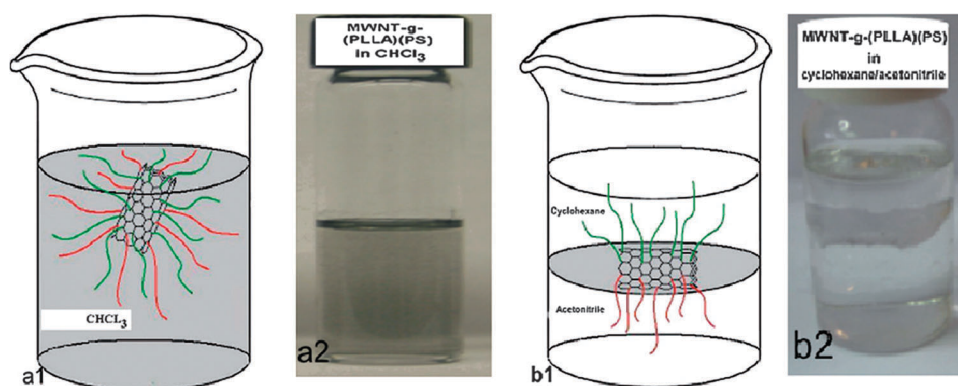
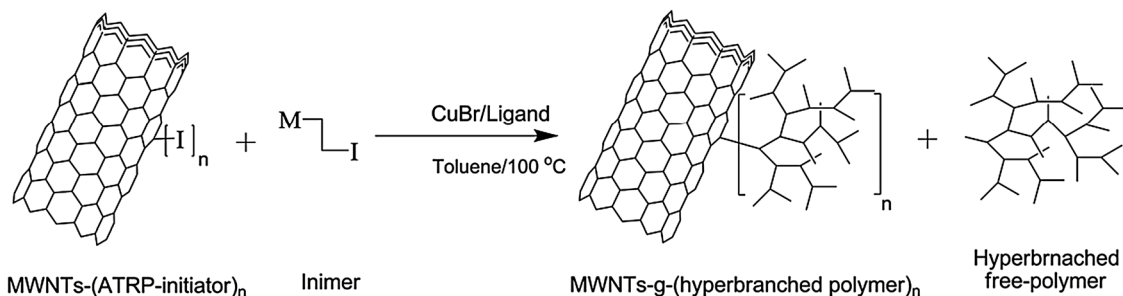


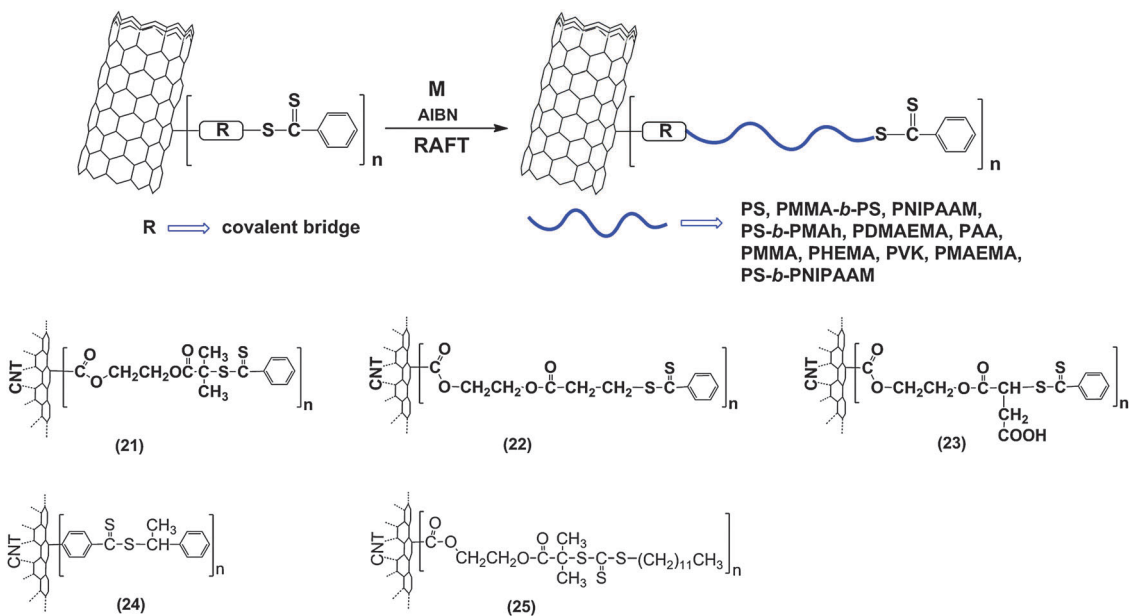
**Fig. 9** (a1) Schematic representation of chemically different grafted brushes (red: PLLA, green: PS) on MWNTs, MWNT-*g*-[(PLLA)<sub>n</sub>(PS)<sub>m</sub>] in CHCl<sub>3</sub>, a good non-selective solvent, (a2) experimental evidence; (b1) schematic representation of MWNT-*g*-[(PLLA)<sub>n</sub>(PS)<sub>m</sub>] in a mixture of selective (bottom layer-acetonitrile for PLLA and top layer-cyclohexane for PS) and immiscible solvents and (b2) experimental evidence. Reprinted with permission from *Soft Matter*, 2009, **5**, 4272.



**Scheme 6** Surface initiated self-condensing vinyl polymerization using ATRP functionalized MWNTs and inimer. Notation for a number of functional groups grafted to the different  $sp^2$  carbons on the CNTs is indicated as a group within a bracket with a number “ $n$ ” for clarity.

**2.1.1.3 Self-condensing vinyl polymerization (SCVP).** Covalent grafting of a linear polymer using ATRP from the CNTs is a straight-forward method as the initiation occurs only from the initiator attached sites on the surface. A concurrent solution polymerization of the monomer, in principle, does not occur to complicate the analysis. In the case of grafting a branched polymer from the CNTs using self-condensing vinyl polymerization by ATRP, the use of inimer introduces complications. Independent solution polymerization of inimer can also proceed in the solution (Scheme 6). Nevertheless, Hong *et al.*<sup>61</sup> polymerized an inimer, 2-((bromobutyl)-oxy) ethyl acrylate, from 2-bromoisobutyrate functionalized MWNTs. As the inimer polymerizes concurrently in the solution, the surface initiated SCVP competes with the solution polymerization. The grafting percentage of the polymer reached 80 wt% and the nanohybrid materials showed good solubility in organic solvents, while the TEM images showed a very thin polymer layer (2–4 nm) around the CNTs. If chosen not to remove the free polymer, one can obtain directly nanocomposites with branched polymer as a matrix.

Linear and hyperbranched glycopolymers were grafted onto MWNTs using 3-*O*-methacryloyl-1,2:5,6-di-*O*-isopropylidene- $\beta$ -glucofuranose (MAIG), and its self-condensing vinyl copolymerization (SCVP) with an inimer, 2-(2-bromoisobutyryloxy)ethyl methacrylate (BIEMA).<sup>62</sup> The kinetic study of the MAIG surface polymerization showed that in the presence of a sacrificial initiator, a first-order time-conversion plot for the polymerization was observed in solution with relatively low polydispersity indices for monomer conversion up to 50%. For higher monomer conversion, a dimerization of freely propagating chains was noticed *via* GPC analysis. Almost identical results were obtained in the absence of a sacrificial initiator. The MWNTs-*g*-PMAIG were deprotected and multihydroxy MWNTs-*g*-PMAG were formed, which were soluble in polar solvents. The content of the grafted hyperbranched glycopolymers was relatively low compared to the linear polymer, which was attributed to a poor initiator efficiency and a cyclization of hyperbranched macromolecules during the SCVP. The degree of branching (DB) of the grafted polymer, as estimated by <sup>1</sup>H-NMR, ranged from 0.49 to 0.21 when the feed mole ratio of monomer to inimer



**Scheme 7** Strategy for covalent attachment of RAFT initiators onto CNTs and polymerization of vinyl monomers. Notation for a number of functional groups grafted to the different  $sp^2$  carbons on the CNTs is indicated as a group within a bracket with a number “ $n$ ” for clarity.

increased from 0.5 to 5. After deprotection, multihydroxy hyperbranched glycopolymer grafted MWNTs were obtained.

**2.1.2 Reversible addition fragmentation chain transfer polymerization (RAFT).** RAFT polymerization is another promising controlled free radical polymerization method that has been used to graft polymers from CNTs (Scheme 7). The reaction is mediated by the reversible addition and fragmentation events in the presence of a dithioester chain transfer agent.<sup>63–65</sup> A small amount of a radical initiator such as azoisobutyronitrile (AIBN) is used to start the reversible chain transfer reaction with dithioester and propagating chains. As the propagation is controlled by the amount of a chain-transfer agent, covalent attachment of an appropriate dithioester on CNTs provides an opportunity to graft vinyl polymers from CNTs.

Cui *et al.*<sup>66</sup> were the first to report the use of RAFT polymerization from MWNTs (Table 1). MWNTs grafted with bromoethyl isobutyrate functionality were transformed into a RAFT agent *via* reacting with Grignard of thionylsulfide. The presence of dithiobenzoate (**21**) on the MNWTs was confirmed by TGA, FT-IR and XPS. The binding energy associated with carbon, oxygen, and sulfur was identified as peaks at 285, 532, 163 eV, respectively (Fig. 10). Polymerization of **S** was performed in the presence of a small amount of AIBN from MWNTs. It was shown that the grafted PS could be controlled by adjusting the monomer to RAFT agent ratio.

Using the same experimental route, Hong *et al.*<sup>67</sup> reported the synthesis of copolymer brush poly(styrene-*alt*-maleic anhydride) on the surface of MWNTs. The highly reactive maleic anhydride groups along the polymer were used for further functionalization with PEO and amino sugar by the *grafting to* strategy. MWNTs-*g*-P(*S-*alt**-MAh) existed as lumpy aggregates and only after broken into powder, the sample was soluble in organic solvents for a short period. The solubility was increased after grafting of PEO on the polymer backbone, in both aqueous and organic solvents. The same behavior was observed when a small amount of amino sugar was grafted onto the copolymer brush instead of PEO. They have also polymerized *N*-isopropylacrylamide from the surface of MWNTs *via* RAFT

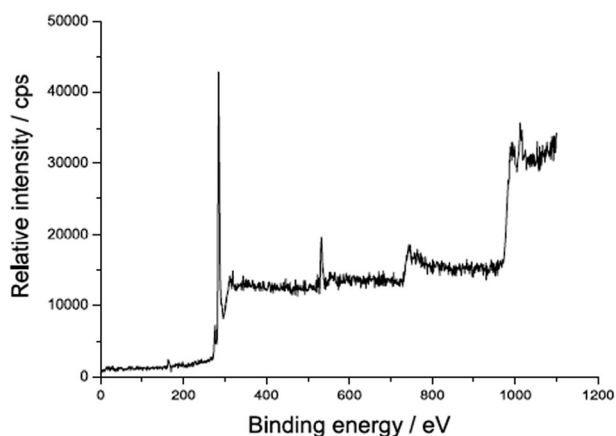


**Fig. 10** XPS of binding energy associated with 0.8 mol% Sulfur at 163 eV along with Oxygen and Carbon elements of MWNTs-*g*-SC(S)Ph. Reprinted with permission from *Polymer*, 2004, **45**, 8717.

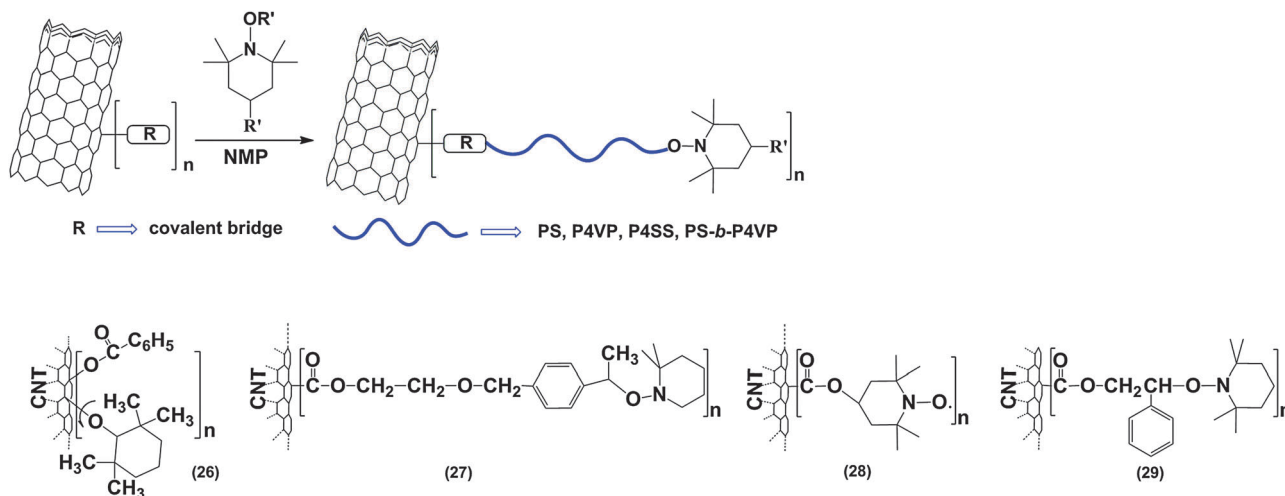
polymerization.<sup>68</sup> TGA results showed around 0.76 RAFT moieties per 100 carbon atoms. The poly(*N*-isopropylacrylamide) (PNIPAM) was cleaved from the surface under basic conditions, and the polymers were further characterized by SEC. The molecular weight of the grafted polymer was relatively low (less than 13 000 g mol<sup>-1</sup>) and increased linearly with the monomer conversion, while the polydispersity indices were in the vicinity of 2.0. The synthesized materials had a PINPAM shell, which was sensitive to temperature changes. At temperatures below the LCST (32 °C) the intermolecular hydrogen bonding of PINPAM with water lead to dispersion, while at temperatures above 32 °C hydrogen bonding between the PNIPAM chains lead to precipitation.

Xu *et al.*<sup>69</sup> showed a reversible two-phase migration behavior of MWNTs-*g*-PNIPAM, which underwent the hydrophilic–hydrophobic transition in water and chloroform mixture solvent. Diblock copolymers of PS and PNIPAM grafted from MWNTs, MWNT-*g*-(PS-*b*-PNIPAM), have been reported to show similar temperature switching behavior.<sup>70</sup> The end groups of the PMMA brushes grafted from the surface of the MWNTs were used to re-initiate **S** to form MWNT-*g*-(PMMA-*b*-PS).<sup>71,72</sup>

You *et al.*<sup>73</sup> covalently grafted a variety of ionic polymers onto MWNTs by RAFT polymerization. Dithioester functionalized MWNTs were used as a RAFT agent for the grafting of a cationic polymer, poly(2-dimethylamino-ethylmethacrylate), an anionic polymer, poly(acrylic acid), and a zwitterionic polymer, poly(3-[*N*-(3-methacrylamidopropyl)-*N,N*-dimethyl] ammonio-propane sulfonate). Water soluble poly(*N*-(2-hydroxypropyl)-methylmethacrylamide) was also grafted from MWNTs *via* RAFT polymerization.<sup>74</sup>

In order to synthesize nanotubes–polymer/Ag hybrid nanocomposite, Pei and co-workers<sup>75</sup> used RAFT polymerization to graft water soluble poly(2-hydroxyethyl methacrylate), PHEMA, from MWNTs. SEC analysis revealed that the length of the PHEMA chains could be controlled with the polymerization time, provided the monomer to dithioester ratio was kept constant. A MWD in the range of 1.4–1.5 was achieved. The PHEMA grafted onto MWNTs was hydrolyzed by HCl to yield poly(methacrylic acid), PMAA, which had a higher loading capacity for metal ions. The carboxyl groups of the PMAA were used to chelate Ag<sup>+</sup> resulting to MWNT-PMAA/Ag nanocomposite materials. They have also reported the synthesis of MWNTs-*g*-PS and studied its application as an additive in base lubricant oil.<sup>76</sup>

Wang *et al.*<sup>77</sup> fabricated water soluble SWNTs by grafting poly(acrylamide) (PAM) *via* RAFT polymerization. In a recent study, Chen and Blau and co-workers<sup>78</sup> studied the non-linear optical properties of MWNTs functionalized with poly(*N*-vinylcarbazole) *via* RAFT polymerization. The grafted polymer content was as high as 96 wt%, and was found to increase with increasing the ratio of monomer to RAFT agent. SEC analysis exhibited molecular weights ranging from 6000 to 22 000 g mol<sup>-1</sup> and MWD close to 1.65. Using UV/Vis spectrum, they revealed that at the same level of linear transmission, the MWNT-PVK with 79.2 wt% of PVK possesses better optical limiting performance than other MWNT-PVK composites, MWNTs and C<sub>60</sub>. This observation was attributed to microplasmas and/or microbubbles, which induce non-linear light scattering.



**Scheme 8** Covalent attachment of different nitroxides for vinyl polymerization. Notation for a number of functional groups grafted to the different  $sp^2$  carbons on the CNTs is indicated as a group within a bracket with a number “ $n$ ” for clarity.

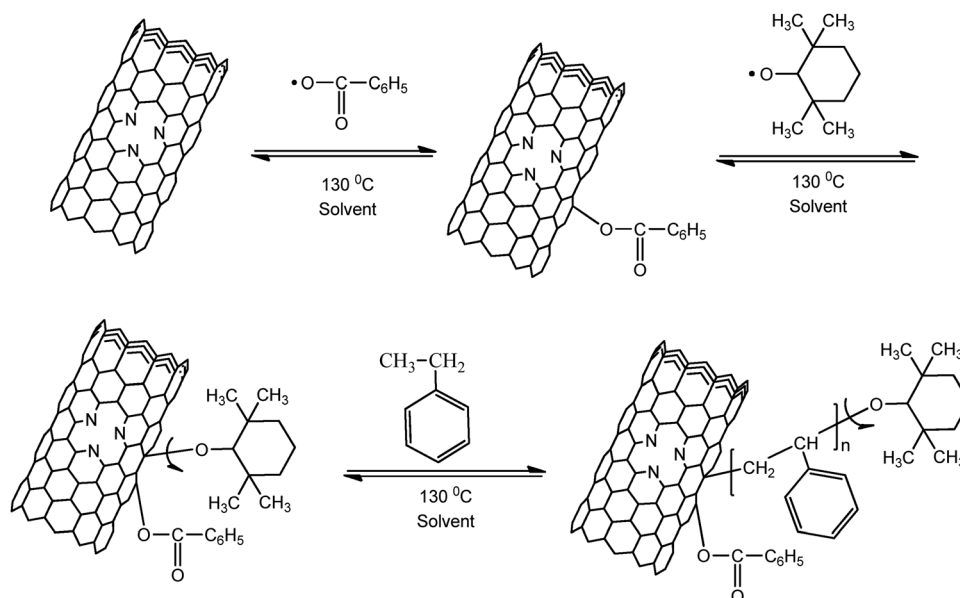
### 2.1.3 Nitroxide mediated radical polymerization (NMRP).

Nitroxide-mediated radical polymerization (NMRP) is another strategy that has been used to grow polymers from CNTs. NMRP is based on a reversible activation and deactivation of active radicals using a stable nitroxide radical.<sup>79</sup> Even though NMRP is considered a valuable method for controlled fabrication of polymer brushes in solution, the number of groups that have used this type of polymerization for grafting polymers from the CNTs are only a few. The monomers used are limited to styrenic and 4-vinyl pyridine. As radicals are generated using conventional thermal radical initiators such as AIBN or benzoyl peroxide (BPO) in NMRP, the transfer mechanism to CNTs is not efficient. Moreover, the transferred radicals are stabilized through  $\pi$ -electrons of the CNTs and thus less efficient for the initiation of vinyl monomer. These factors may reduce the

efficiency of NMRP and thus, are not effectively used in SIP from CNTs (Scheme 8).

*In situ* NMRP was used for the synthesis of polystyrene from the surface of  $N$ -doped MWNTs ( $CN_x$ ).<sup>80</sup> The grafting reactions were carried out in a two-step process (Scheme 9). The  $N$ -doped MWNTs were functionalized with a free-radical initiator, benzoyl peroxide (BPO), creating a resonance stabilized radical that was used to trap the nitroxide reagent,  $NO_x$ , and generate macroinitiators for the polymerization. Using MWNTs-nitroxide (26), the polymerization of S was performed.

Zhao *et al.*<sup>81</sup> reported the functionalization of CNTs with poly(4-vinylpyridine), P4VP, and poly(sodium 4-styrenesulfonate), PSS, and their solubility at different pH values. Acid chloride activated CNTs were treated with hydroxyl functionalized TEMPO for the generation of the macroinitiator (27). The authors showed



**Scheme 9** Functionalization of  $CN_x$  with benzoyl peroxide and nitroxide controller, (26), and surface initiated NMRP of styrene.



that the content of the grafted polymer increased with increasing the ratio of monomer to initiator. The interaction of the pyridine groups of the MWNTs-*g*-P4VP with acid produced a good dispersion in aqueous solution. The MWNTs-*g*-PSS showed an excellent dispersion in both acidic and in basic conditions depending on its acid and sodium salt form, respectively.

Similarly, TEMPO-functionalized MWNTs were used to grow polystyrene by NMRP in a controllable way.<sup>82</sup> The MWNTs-*g*-PS could initiate the polymerization of 4-vinyl pyridine in order to form block copolymer grafted MWNTs. Fan *et al.*<sup>83</sup> attached free TEMPO-OH radicals on carbonyl chloride functionalized MWNTs (28), and synthesized PS brushes. The polymerization was performed in the presence of a small amount of free-initiator.

Chang *et al.*<sup>84</sup> attached TEMPO-OH at two different batches of MWNTs having average diameters of 5 and 10–25 nm, respectively, and used them for bulk polymerization of styrene. They observed that after grafting PS a large diameter tubes were easy to dissolve, compared to smaller diameter tubes that were less dispersible.

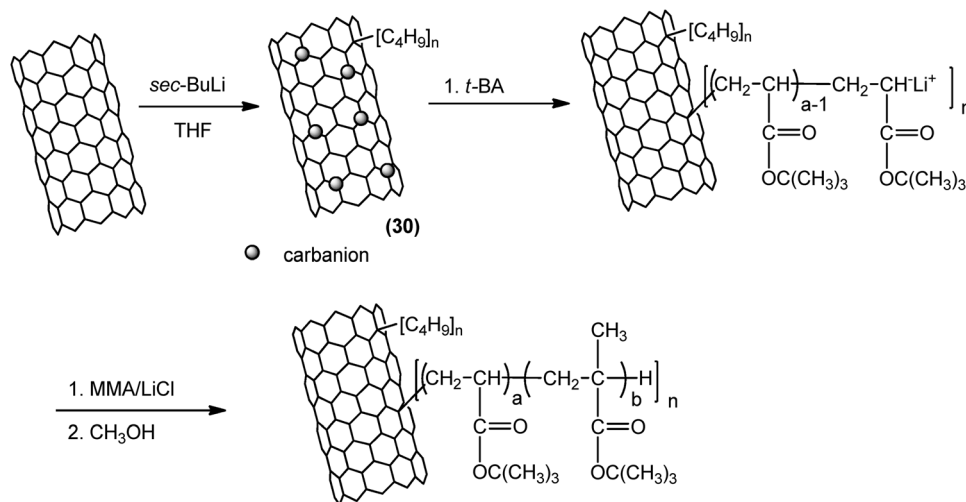
**2.1.4 Anionic polymerization.** The most important drawback of surface initiated controlled radical polymerization from CNTs is that the process does not provide adequate control of the molecular weight of the grafted polymer. The limiting factors are the side reactions associated with the intermediate radicals, intramolecular coupling and stability at very low concentration. However, the living nature of anionic polymerization<sup>85</sup> with its ability to afford polymers of MWD and high molecular weight in a controlled way, even at very low initiator concentration, has made it an attractive choice in grafting polymers from CNTs. This section will deal with the anionic polymerization of vinyl monomers such as styrene and (meth)acrylates from CNTs.

Viswanathan *et al.*<sup>86</sup> were the first to grow polymers from nanotubes *via* anionic polymerization. They introduced carbanions on the surface of the SWNTs through addition of *sec*-butyllithium (*sec*-BuLi) to the  $sp^2$  carbons. The resulting resonance stabilized carbanion on the SWNTs was used as the initiating site for the polymerization of S. It was stated that a mutual electrostatic

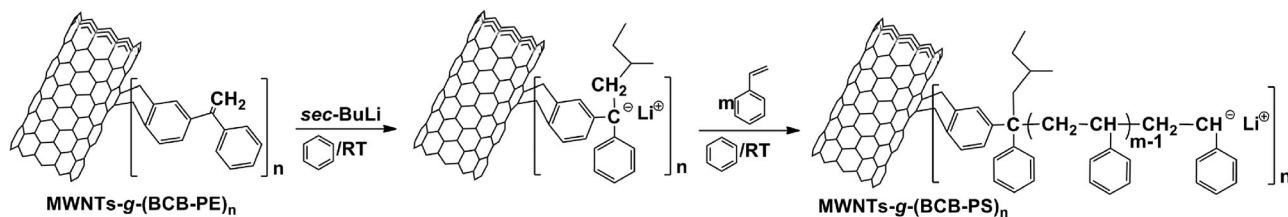
repulsion between the individual nanotubes was able to exfoliate the SWNT bundles. The amount of carbanion generated on the SWNTs was not determined as the S polymerization was conducted *in situ* in the presence of free *sec*-BuLi. Thus, a concurrent solution polymerization produced PS nanocomposite consisting of MWNTs-*g*-PS. Grafting efficiency was determined after removing the free PS from MWNTs-*g*-PS through a solvent wash by TGA, and it was found to be very low (~10–15 wt%). The observed  $T_g$  of the grafted PS in MWNTs-*g*-PS was higher by 15 °C than neat PS. Using the same approach (30), Chen *et al.*<sup>87</sup> showed that the carbanions on the surface of SWNTs could also initiate the polymerization of *tert*-butyl acrylate (*t*-BA) but not that of methyl methacrylate (MMA). The authors suggested that a possible reason for this behavior was the difference in the reactivity of the two monomers towards the delocalized carbanions on the SWNTs. However, it must be noted that Ajayan *et al.* showed the reactivity of the generated carbanions on the SWNTs was sufficient enough to initiate S.<sup>86</sup> Thus, the reactivity difference of the monomers cannot be the reason for the observed behavior. Nevertheless, the authors confirmed the living nature of the polymerization by initiating MMA from the growing PtBA enolate anions. The same group synthesized a diblock copolymer (PtBA-*b*-PMMA) from SWNTs with 47 wt% polymer (Scheme 10).

In contrast, Liang *et al.*<sup>88</sup> reduced SWNTs in the presence of Li in ammonia as anionic initiators for the polymerization of MMA. They showed that an addition of Li/NH<sub>3</sub> to SWNTs leads to SWNTs salts that have the ability to exfoliate SWNTs bundles and grow PMMA. The CNTs with 45 wt% polymer were synthesized and the average thickness of the amorphous polymer layer around the SWNTs was 1.0–1.5 nm, as calculated by AFM.

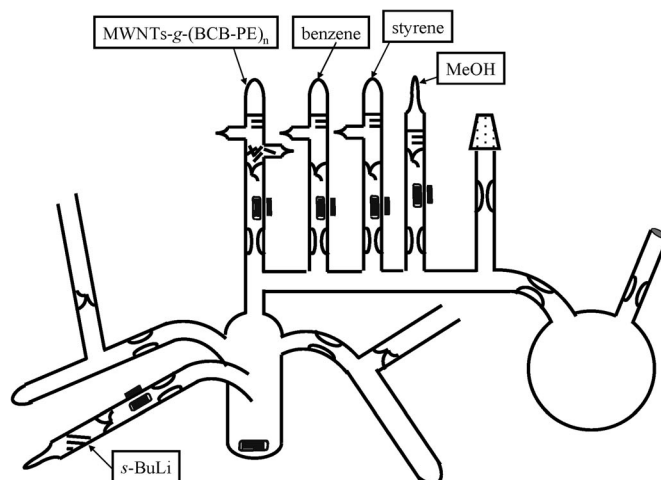
In order to achieve a higher grafting efficiency and a higher molecular weight, Baskaran and co-workers used a different approach<sup>89</sup> to grow PS from MWNTs *via* anionic polymerization. As mentioned previously, the direct reaction of *sec*-BuLi with the  $sp^2$  carbon of MWNTs was inefficient.<sup>86,90</sup> Therefore, they generated carbanion sites away from the CNTs surface.



**Scheme 10** Anionic polymerizations of methyl acrylate and methyl methacrylate from SWNTs and SWNT-*g*-(PtBA), respectively. Notation for a number of functional groups grafted to the different  $sp^2$  carbons on the CNTs is indicated as a group within a bracket with a number “*n*” for clarity.



(32)



**Scheme 11** Anionic polymerization of styrene from MWNTs-*g*-(BCB-PE) grafted tubes in benzene at RT and the reactor used for the polymerization. Notation for a number of functional groups grafted to the different  $sp^2$  carbons on the CNTs is indicated as a group within a bracket with a number "n" for clarity.

Accordingly, the MWNTs were covalently functionalized with 1-benzocyclobutene-1'-phenylethylene (BCB-PE) through a [4 + 2] Diels-Alder cycloaddition (32).<sup>91</sup> A statistical distribution of covalent attachment of substituted diphenylethylene, a precursor initiator, was introduced throughout the surface of MWNTs. The presence of the olefin was confirmed by FT-IR, Raman spectroscopy, and TGA. Reactive carbanions were generated from MWNTs-*g*-(BCB-PE)<sub>n</sub>, by addition of *sec*-BuLi. The polymerization of S was initiated in benzene at room temperature under high-vacuum conditions (Scheme 11). The typical red color of the phenylhexyllithium anion on the MWNTs was not seen, probably due to an intense black color of the solution, resulting from the gradual dispersion of PS grafted MWNTs. The initiation of S from the surface grafted phenylhexyllithium anions was found to be slow. This was attributed to the heterogeneous nature of the reaction. A small amount of MWNTs-*g*-initiator was insoluble in the reactor during the polymerization for about an hour. On the other hand, the polymerizations carried out for more than 90 min showed a complete dispersion of MWNTs during the polymerization. The surface grown polymers were obtained in high conversion, forming MWNTs-*g*-PS containing only a small fraction of MWNTs (<1 wt%). A control polymerization of S was carried out using *sec*-BuLi in the presence of pristine MWNTs. Upon addition of S, an orange color appeared immediately indicating the initiation of S from the free initiator present in the solution. After the termination of the polymerization, the MWNTs were recovered by a thorough solvent-wash in THF to remove free PS. The recovered MWNTs did not have grafted PS as confirmed by TGA and TEM analysis.

The MWNTs-*g*-PS were characterized by FT-IR, <sup>1</sup>H-NMR, Raman spectroscopy, DSC, TGA, and TEM. The TEM images showed the presence of a thick layer of polymer (~30 nm) around the surface of MWNTs (Fig. 11). The formation of diblock copolymer, MWNTs-*g*-(PS-*b*-PI) confirmed the living nature of the polymerization.

## 2.2 Application of ring-opening polymerizations

Aliphatic polyesters, such as poly(*p*-dioxanone), poly( $\epsilon$ -caprolactone), poly(*t*-lactide), polyethers (*e.g.* PEO) and polypeptides, are biocompatible and in most cases biodegradable polymers. These materials have been proven to be very useful in implantable medical devices, as surgical sutures and in drug-delivery systems, since they eliminate the need for removal of the device after being used. Their synthesis involves ROP techniques.<sup>92</sup> Grafting polyether, polyamide and polyester from CNTs is very important (Table 2) as these materials can be used as fillers in developing nanocomposites in commodity plastics to enhance the mechanical property. The ROP can be performed by several initiating systems such as anionic, cationic, coordination, and metathesis.

### 2.2.1 Anionic-coordination polymerization

**2.2.1.1 Grafting polyglycidol and polydioxanone.** Yoon *et al.*<sup>93</sup> used ROP to graft poly(*p*-dioxanone) (PPDX) from SWNTs *via* the *grafting from* method. The surface of SWNTs was covalently attached with 6-amino-1-hexanol by immersing the acid chloride-functionalized SWNTs into dimethyl formamide (DMF). The produced hydroxy-functionalized SWNTs-(OH)<sub>n</sub> were then used

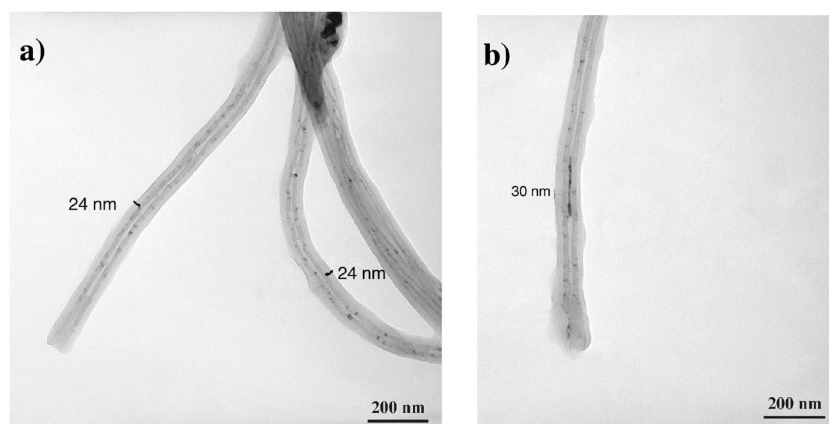


Fig. 11 TEM images of surface-grown PS exhibiting up to 30 nm PS layer on the surface of MWNTs. Reprinted with permission from *Chem. Mater.*, 2008, **20**, 6217.

Table 2 ROP polymerization (anionic-coordination, cationic, metathesis)

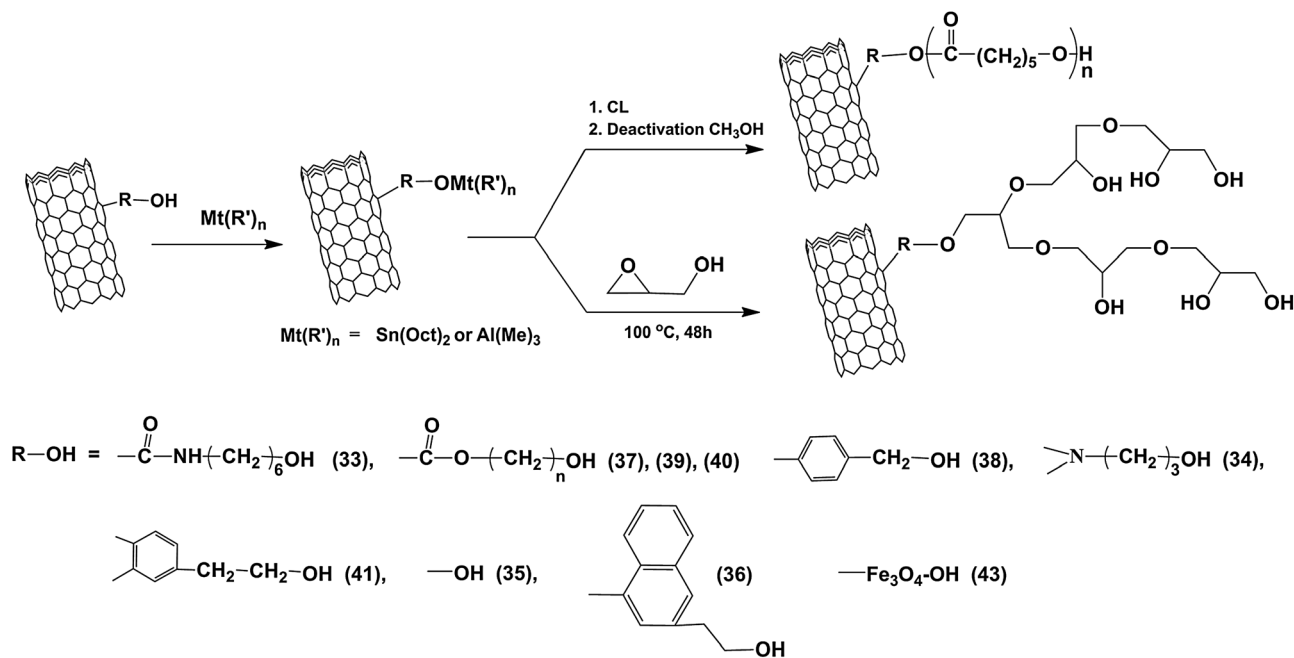
Type of CNTs	Initiator functionality	Monomer <sup>a</sup>	Catalyst	Solvent/temperature/time	[I] <sub>0</sub> <sup>b</sup> (×10 <sup>5</sup> mol)	[M] <sub>0</sub> mol L <sup>-1</sup>	wt% Grafted <sup>c</sup> polymer	Ref.
Polymerization: anionic-coordination								
SWNTs	(33)	<i>p</i> -Dioxanone	Sn(Oct) <sub>2</sub>	Toluene/90 °C/72 h	—	0.5	40	93
MWNTs	(41)	EO	—	THF/50 °C/48 h	1.11	6.29	96	89
MWNTs	(38)	ε-CL	Sn(Oct) <sub>2</sub>	DCB/130 °C/24 h	—	1.24	63	99
MWNTs	(37)	ε-CL	Sn(Oct) <sub>2</sub>	Bulk/120 °C/24 h	14.2	—	32–52	100
MWNTs	(39)	ε-CL	Al(CH <sub>3</sub> ) <sub>3</sub>	Toluene/RT/18 h	—	8.76	95–99	101
MWNTs	(40)	ε-CL	Al(CH <sub>2</sub> CH <sub>3</sub> ) <sub>3</sub>	Toluene/40 °C /25 min	—	—	—	102
MWNTs	(34)	ε-CL	Sn(Oct) <sub>2</sub>	DCB/120 °C/16 h	1.9	0.45	58	103
MWNTs	(41)	ε-CL	Sn(Oct) <sub>2</sub>	THF/120 °C/3 min–4 h	0.6	4.0	18–98	105, 106
SWNTs	(44)	ε-Caprolactam	Na	Bulk/140 °C/24 h	2.5	—	30	117
MWNTs	(45)	ε-Caprolactam	Na	Bulk/170 °C/2–10 h	1.5	—	40–65	118
MWNTs	(35)	Glycidol	CH <sub>3</sub> O <sup>-</sup> K <sup>+</sup>	Bulk/100 °C/4 h	—	—	56	95
MWNTs	(34)	Glycidol	CH <sub>3</sub> <sup>-</sup> K <sup>+</sup>	Dioxane/95 °C/4 h	—	5.69	21–91	94
MWNTs	(37)	L-LA	Sn(Oct) <sub>2</sub>	DMF/140 °C /2–20 h	—	0.2	10–35	107
		ε-CL	“	“	“	“	“	108
		“	“	“	“	“	“	109
		α-chloro-ε-CL	“	“	“	“	34–86	98
MWNTs	(43)	L-LA	Sn(Oct) <sub>2</sub>	Bulk/130 °C/48 h	—	—	26–34	111
MWNTs	(37)	L-LA	Sn(Oct) <sub>2</sub>	Toluene/130 °C/48 h	3.9	—	73	112
		ε-CL	“	“	“	“	“	“
SWNTs	(42)	L-LA	—	Toluene/135 °C/7.5–20 h	0.6	5.6	13–94	110
MWNTs		ε-CL	—	Toluene/120 °C/20 h	1.2	6.8	78	“
		<i>n</i> -HIC	—	Toluene/RT/20 h	1.7	10.3	—	“
MWNTs	(44)	ε-Boc-L-Lys-NCA	—	THF/30 °C/48 h	5.0	0.10	27–54	115
SWNTs	(43)	γ-BLG-NCA	—	DMF/RT/48 h	5.5	0.19	41	114
MWNTs	(34)	ε-CL	Sn(Oct) <sub>2</sub>	Bulk/120 °C/24 h	8.9	—	42	96
MWNTs	(36)	L-LA	Sn(Oct) <sub>2</sub>	Toluene/110 °C/24 h	2.6	0.37	40	97
		ε-CL	“	“	“	“	“	“
Polymerization: cationic								
MWNTs	(37)	EHOX	BF <sub>3</sub> Et <sub>2</sub> O	CH <sub>2</sub> Cl <sub>2</sub> /–10 °C/24 h	13.4	0.86	20–87	121
MWNTs	(46)	ECP	FeCl <sub>3</sub>	Bulk/RT/12 h	—	—	40	122
Polymerization: metathesis								
SWNTs	(47)	Norbornene	—	CHCl <sub>3</sub> /RT/5–180 min	—	0.353	—	124

<sup>a</sup> ε-CL: ε-Caprolactone, L-LA: L-Lactide, EO: Ethylene Oxide, *n*-HIC: *normal*-Hexyl Isocyanate, EHOX: Ethyl Hydroxymethyl Oxetane, ECP: Epoxychloro Propane, γ-BLG-NCA: γ-Benzyl-L-Glutamate *N*-Carboxyanhydride, and Boc-L-Lys-NCA: ε-(Benzoyloxycarbonyl)-L-Lysine *N*-Carboxyanhydride. <sup>b</sup> Moles of initiator present on the total grams of CNTs in the reaction. <sup>c</sup> Determined by TGA with respect to carbon. (—) Data not available.

for the initiation of *p*-dioxanone, in the presence of tin(II) 2-ethylhexanoate (Sn(Oct)<sub>2</sub>). They found that the thermal stability of the grafted PPDX increased after the covalent attachment onto the SWNTs. The SWNTs-*g*-PPDX had no noticeable transition corresponding to *T*<sub>g</sub> and *T*<sub>m</sub> up to 125 °C, although pure PPDX showed these transitions at –13.4 and 103 °C, respectively. The changes in

the grafted PPDX properties were attributed to a strong interaction between SWNTs and PPDX and a decreased mobility of the PPDX chains.

Gao's group<sup>94</sup> performed anionic ROP of glycidol (2,3-epoxy-1-propanol) in dioxane using potassium methoxide as a catalyst, to grow hyperbranched polyglycerol (HPG) from



**Scheme 12** Synthesis of MWNT-*g*-PCL and MWNTs-*g*-HPG using different types of initiators *via* anionic coordinative ring-opening polymerization.

MWNTs-(OH)<sub>*n*</sub> surfaces. The macroinitiator, MWNT-OH, was prepared by reacting with 2-azidoethanol in *N*-methyl-2-pyrrolidone (34). The amount of grafted HPG was adjusted, up to 90 wt%, by changing the feed ratio of glycidol to MWNTs-(OH)<sub>*n*</sub>. When the polymerization was conducted in bulk, the grafted polymer content was never higher than 45 wt%, even at high feed ratios of glycidol to MWNTs-(OH)<sub>*n*</sub>. The authors ascribed this phenomenon to the higher viscosity of the reaction mixture in the bulk polymerization. In fact, an extended aggregation of propagating center with potassium counter ion and a lack of solvation of counter ion could be the other reason for poor conversion of HPG in the absence of solvent. A concurrent self-condensing ROP of glycidol through counterion exchange to the monomer was monitored. The number average molecular weights of the free HPGs increased linearly with increasing the feed ratio of monomer to initiating site, and the polydispersity indices were relatively low (<1.8). Although the authors claimed that the polymerization had a living character, such a high MWD confirms that the polymerization proceeded with severe side reactions in the presence of CNTs. The HPG grafted MWNTs (MWNTs-*g*-HPG) were recovered by dispersion in methanol, followed by centrifugation and washing several times with excess methanol. The remaining solid, MWNTs-*g*-HPG, was dried overnight. By reacting to the hydroxy groups of the grafted HPG with palmitoyl chloride, they produced MWNTs-*g*-amphiphilic hyperbranched polymers. The resulting product showed good solubility in weak polar or non-polar solvents in contrast to MWNTs-*g*-HPG, which were soluble only in strong polar solvents. Fluorescent MWNTs were also prepared by attaching rhodamine 6B molecules to the surface of MWNT-*g*-(HPG). The abundance of functional groups on the surface of CNTs hybrids can be used as a nanoplatfrom to

conjugate functional molecules for further application in drug delivery, cell imaging and bioprobng.

Another route for the synthesis of biocompatible and biodegradable CNTs hybrids was reported by Adeli *et al.*<sup>95</sup> Hyperbranched molecular trees were grown from the surface of MWNTs *via in situ* anionic ROP of glycidol as described below (Scheme 12). Short-term *in vitro* cytotoxicity and hemocompatibility tests were conducted on HT 1080 cell line (human Fibrosarcoma) for MWNTs-*g*-HPG. The results showed no sign of toxicity for concentrations up to 1 mg mL<sup>-1</sup> after 24 h of the incubation.

**2.2.1.2 Grafting poly( $\epsilon$ -caprolactone).** Several methods have been reported to introduce a hydroxyl group on CNTs for the polymerization of  $\epsilon$ -caprolactone and other monomers using ROP.<sup>96–98</sup> The reaction of pristine MWNTs with various azide compounds *via* 1, 3-cycloaddition,<sup>96</sup> the use of diradicals *via* Bergman cyclization,<sup>97</sup> and the conversion of acid groups of MWNTs to azide for copper catalyzed Huisgen's 1, 3-dipolar cycloaddition<sup>98</sup> with various functional alkynes are a few of these methods.

Buffa *et al.*<sup>99</sup> functionalized SWNTs produced by the CoMo-CAT process with 4-hydroxymethylaniline (HMA) *via* the diazonium salt method (38). The SWNTs-(OH)<sub>*n*</sub>, generated by the functionalization were then used to polymerize  $\epsilon$ -caprolactone, in the presence of stannous octanoate as the catalyst. The dispersion of SWNTs grafted with poly( $\epsilon$ -caprolactone) (PCL) was tested in chloroform. A dramatic increase compared to that of neat SWNTs was observed due to the high solubility of PCL in chloroform. TGA of the samples indicated that the amount of PCL grafted was 63 wt%, while a combined TPD (temperature-programmed desorption)/TPO (temperature-programmed



oxidation) technique revealed that the average polymer length was only 5 monomeric units. According to the authors, the two main factors for the limited growth of the grafted chains were the presence of nanotubes in the polymerization medium and the presence of adsorbed water on the CNT surface. The former acts as terminator while the latter as initiator generating a large amount of 'free' PCL. Accordingly, it was suggested that an increase in the length of the PCL attached to the nanotubes can only be achieved when the adsorbed water from the nanotubes is eliminated.

In a similar work,<sup>100</sup> the hydroxyl groups were introduced on the MWNT surfaces by reacting oxidized MWNTs with excess thionyl chloride and then with glycol. The  $-OH$  functionalized MWNTs were used for the surface initiated ROP of  $\epsilon$ -caprolactone, in butanol at 120 °C in the presence of stannous octanoate. The content of the grafted polymer and the molecular weight of the free polymer initiated by the butanol were increased with increasing the feed ratio of the monomer to initiating sites. The polydispersity indices of the free polymer were very broad reaching even 13.0, which was ascribed to the increased possibility of chain termination due to the presence of the CNTs. However, the actual mechanism of the propagating PCL anion undergoing termination with the  $sp^2$  carbon network was not discussed. Biodegradation of the recovered MWNT-*g*-PCL was tested by using pseudomonas lipase as a bioactive enzyme catalyst. It was revealed that the grafted PCL chains retained their biodegradability and were completely degraded within 4 days. In contrast, PS lipase and MWNTs had no strong effect on each other.

The influence of MWNT-*g*-PCL on vapor sensing properties was investigated, by Castro *et al.*,<sup>101</sup> for a series of Conductive Polymer Composite (CPC) transducers. MWNTs-*g*-PCL were prepared by first reacting MWNTs-(OH)<sub>*n*</sub> with trimethylaluminium (catalyst) (39) to produce an intermediate compound, followed by the anionic coordination ROP of  $\epsilon$ -caprolactone (see Section 2.2.1.1, Scheme 12). AFM observations allowed an evaluation of the MWNT coating and dispersion levels. Sensors were prepared by spraying layer-by-layer MWNTs-*g*-PCL solutions onto the interdigitated copper electrodes that had been etched by photolithography onto an epoxy substrate. Chemo-electrical properties of CPC sensors exposed to different vapors: water, methanol, toluene, tetrahydrofuran and chloroform were analysed in terms of signal sensitivity, selectivity, reproducibility and stability. The MWNTs-*g*-PCL sensors displayed a very good discrimination capability for all the vapors above (polar and non-polar), which allowed for the preparation of sensors with a large detection spectrum. The chemo-electrical properties of the sensors exposed to different vapors were found to be reproducible, and the electrical signals displayed reversibility with a fast recovery.

A different synthetic approach for the grafting of  $\epsilon$ -caprolactone on MWNTs was presented by Ruelle *et al.*<sup>102</sup> MWNTs were placed under an atomic nitrogen flow formed by the dissociation of molecular nitrogen in Ar + N<sub>2</sub> mixed microwave plasma, in order to covalently functionalize with primary and secondary amines. The amino-MWNTs were activated by triethylaluminium and then used as an initiator for ROP of  $\epsilon$ -caprolactone. As revealed by TEM, functionalization was inhomogeneous and the MWNTs had a high percentage (10 at% N) of

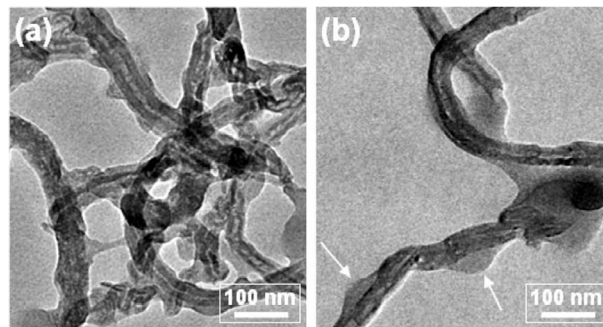
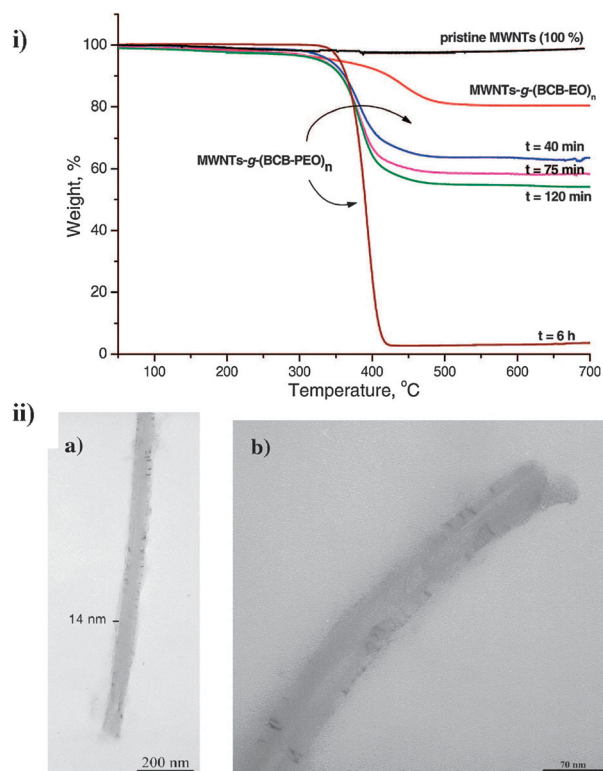


Fig. 12 TEM images of MWNTs-*g*-PCL complexed with  $\alpha$ -CDs. Reprinted with permission from *Eur. Polym. J.*, 2010, **46**, 145.

amine functionalization on the plasma exposed surface of the sample.

Biodegradable supramolecular hybrids of MWNT-*g*-PCL and  $\alpha$ -cyclodextrins ( $\alpha$ -CDs) (inclusion complexes), with potential applications in medicine and biology, were prepared by Y. Yang *et al.*<sup>103</sup> First, MWNTs were functionalized with hydroxyl groups (MWNTs-(OH)<sub>*n*</sub>) *via* a nitrene cycloaddition with an appropriate reagent (34). The reaction was followed by the surface initiated ROP of  $\epsilon$ -caprolactone in the presence of a metal catalyst to afford MWNTs-*g*-PCL. TGA showed about 58 wt% of PCL was grafted onto the MWNTs and TEM images revealed the presence of polymer layers with thicknesses in the range of 5–7 nm on the surface of the MWNTs. Inclusion complexes were formed by hydrogen bonds between the hydroxyl groups of  $\alpha$ -CDs and the carbonyl groups of PCL, indicating that supramolecular polypseudorotaxanes were formed through  $\alpha$ -CD channel threading onto the PCL chains of MWNT-*g*-PCL (Fig. 12). However, the size of uneven pimples shown in Fig. 12 was very large that it could not be interpreted only for supramolecular polypseudorotaxanes formation. It is important to mention that the  $\alpha$ -CD is also known to get adsorbed onto the CNTs.<sup>104</sup> Therefore, the contribution of adsorption and its influence on the reported results are not known.

**2.2.1.3 Grafting poly(ethylene oxide).** In order to achieve higher efficiency of grafting and to graft high molecular weight polymers, Baskaran and co-workers used anionic polymerization approach.<sup>89</sup> They polymerized ethylene oxide (EO) *via* anionic ROP from MWNTs functionalized with hydroxyl groups. The MWNTs were first covalently functionalized with 4-hydroxyethyl benzo-cyclobutene (BCB-EO) through [4 + 2] Diels-Alder cycloaddition. The attachment of the BCB-EO, a hydroxyl precursor, was confirmed by FT-IR, Raman spectroscopy, and TGA. Triphenylmethyl potassium was used to convert the hydroxyl groups on the surface of MWNTs into alkoxide anions. As alkoxide anions exist in rapid equilibrium with the remaining hydroxyl groups, a minimum of 30 mol%, hydroxyls was converted into alkoxide anions. The initiation of ethylene oxide from the surface alkoxy-anions was very slow. The heterogeneous nature of the reaction and the aggregation of alkoxide anions in the presence of MWNTs were attributed to a slow propagation. However, at a constant mole ratio of monomer to grafted initiator, the amount of grafted poly-ethylene oxide (PEO) increased gradually with increasing the



**Fig. 13** (i) TGA kinetic plot of the surface initiated polymerization of PEO from MWNTs, and (ii) TEM images of MWNTs-g-PEO (a and b). Reprinted with permission from *Chem. Mater.*, 2008, **20**, 6217.

polymerization time (Fig. 13i). The monomer conversion also increased gradually with polymerization time reaching a maximum of 57% after 48 hours, indicating a slow propagation of the surface polymerization. Surface-grown polymers were obtained in high conversion, forming MWNTs-g-PEO containing only a small fraction of MWNTs < 4 wt%.

For samples obtained after a long polymerization time, it was not possible to filter the reaction solution through a Teflon membrane, and the samples were recovered by precipitation in non-solvent. SEC analysis, using light scattering detector, of these samples showed the presence of multiple peaks. This was attributed to the fact that MWNTs are broadly distributed in terms of length, diameter, and also chemical functionalization. Although these samples could be analyzed using SEC, with styrene-divinylbenzene crosslinked gel columns, an efficient resolution of different molecules based on the size is not possible. The hydrodynamic volume of MWNTs-g-PEO is expected to be very high as the tubes are very long, and most of them will pass through interparticle gaps rather than getting into the pores. Therefore, such an analysis would only give an apparent molecular weight that can be used for a relative comparison within a set of experiments. One must be cautious in treating the SEC data of polymer grafted CNTs due to the reasons mentioned above. Nevertheless, the MWNTs-g-PEO samples taken at different polymerization time showed (in SEC) an increase in apparent molecular weight indicating overall control on the molecular weight of the grafts is possible in these reactions. A light

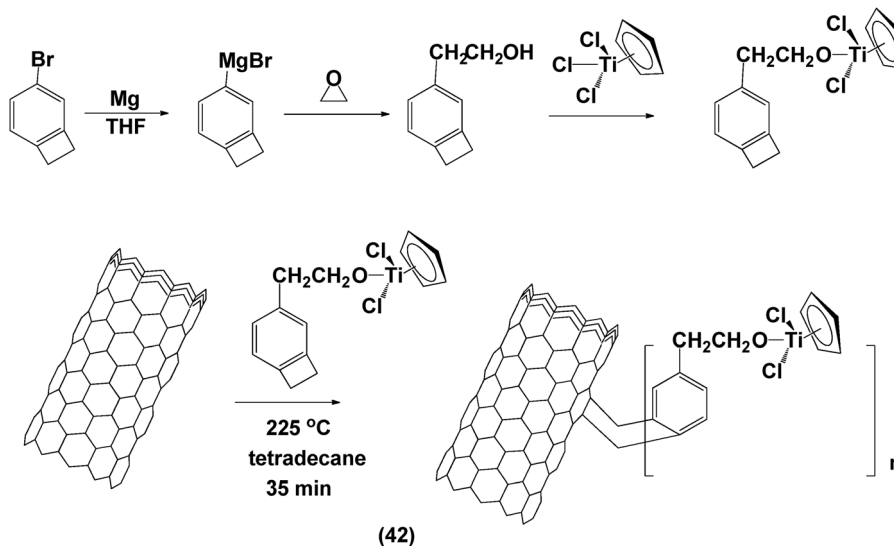
scattering detector showed multiple peaks corresponding to a few thousands to a few millions in weight average molecular weight, confirming the presence of multiple distributions of high molecular weight species. The TEM images showed the presence of thick layers of grafted PEO, non-uniformly distributed along the whole surface (Fig. 13ii).

Very recently, our group<sup>105</sup> studied the kinetics of ROP of  $\epsilon$ -CL from MWNT and the crystallization behavior of MWNTs-g-PCL together with that of MWNTs-g-PEO. The polymerization could be controlled with time, though the reaction proceeded rapidly. As revealed by TGA, a 98 wt% of PCL was grafted after 4 h and 70% monomer conversion was achieved. A remarkable nucleation effect was observed by the incorporation of MWNTs, which reduced the supercooling needed for crystallization of both PCL and PEO. Furthermore, the isothermal crystallization kinetics of the grafted PCL and PEO were substantially accelerated compared to the neat polymers, which were attributed to the anchoring of the chain-ends to the MWNTs *via* covalent bonding.

In another study in our laboratory,<sup>106</sup> diblock copolymers were grafted onto MWNTs *via* a combination of polymerization techniques. Using the same method above, a substituted benzocyclobutene containing hydroxyl group was attached on the surface of MWNTs and later used for the polymerization of EO or  $\epsilon$ -CL. The hydroxyl groups of the grafted polymer chain-ends were used for the initiation of the second block. Accordingly, the chain-ends of the MWNTs-g-PEO were used as a ROP macroinitiator for the polymerization of  $\epsilon$ -CL resulting in biocompatible MWNT-g-(PEO-*b*-PCL). By esterification of the hydroxyl PEO end groups with excess 2-bromoisobutyl bromide, an ATRP macroinitiator was obtained and used for the polymerization of S and 2-(dimethylamino)ethylmethacrylate (DMAEMA) resulting in diblock copolymer grafted MWNTs, which had very high (>90 wt%) grafted polymer content. This strategy, through a combination of two different polymerization techniques, widens the opportunities for the synthesis of even more complex macromolecular structures on the CNTs surface.

**2.2.1.4 Grafting polylactide.** Poly(L-lactide) (PLLA) is widely used in tissue engineering, drug-delivery systems and implant materials due to its excellent biocompatibility and biodegradability. However, the mechanical properties of PLLA for high load bearing biomedical applications are insufficient. PLLA nanocomposite containing CNTs has been implied to enhance the mechanical properties for various applications. The first attempt to polymerize L-lactide from the surface of MWNTs was reported by Chen *et al.*<sup>107</sup> Carboxylic acid functionalized MWNTs were treated with  $\text{SOCl}_2$  and the acyl chloride containing CNTs were further reacted with butanediol, in order to introduce hydroxyl groups on the surface. The polymerization of L-lactide was performed in the presence of stannous octanoate. The amount of grafted PLLA increased with time depending on the polarity of the reaction medium. When the polymerization was carried out in DMF, the amount of grafted PLLA on the MWNTs was higher than that obtained in toluene.

Nanocomposites of PLLA with MWNTs-g-PLLA were prepared and tested for mechanical property enhancement. The



**Scheme 13** Grignard synthesis of (1-benzocyclobutene ethoxy) dichlorocyclopentadienyltitanium (BCB-EOTiCpCl<sub>2</sub>) and covalent functionalization of MWNTs using a [4 + 2] Diels–Alder cycloaddition reaction. Notation for a number of functional groups grafted to the different sp<sup>2</sup> carbons on the CNTs is indicated as a group within a bracket with a number “n” for clarity.

authors claimed that the incorporation of 1 wt% of MWNT-*g*-PLLA into the PLLA matrix did not show any indication of aggregation based on SEM, and the nanocomposites exhibited high tensile-strength and modulus rendering PLLA more resistant to deformation. Thermal stability, electrical conductivity as well as mechanical properties of PLLA nanocomposites containing MWNT-*g*-PLLA were also studied.<sup>108,109</sup> Good interfacial adhesion between MWNTs and the polymer matrix in PLLA/MWNT-*g*-PLLA composites also increased the activation energy compared to PLLA/MWNT, indicating that the former was thermally more stable.

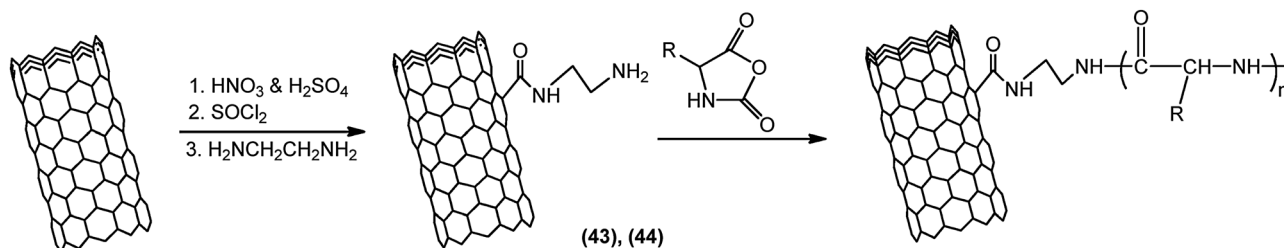
Recently, our group<sup>110</sup> used a titanium alkoxide catalyst (–TiCpCl<sub>2</sub>) to polymerize *L*-lactide,  $\epsilon$ -CL and *n*-hexyl isocyanate from SWNTs and MWNTs (42). A Diels–Alder cycloaddition was used to covalently attach benzocyclobutene functionalized with titanium alkoxide, to the sidewalls of CNTs (Scheme 13). The grafted CNTs were used for the titanium-mediated SIP of different monomers. Kinetic study of the *L*-LA polymerization indicated that the initiation was very slow and characterized by an induction period of about 4 h. After this period, the polymerization medium became homogeneous and the polymerization proceeded fast giving enhanced efficiency for grafting polymers on the CNTs. The viscosity of the reaction medium was substantially increased the next 5 h. The long induction period could be attributed to a steric hindrance of MWNTs-titanium complex for the initiation. Titanium-mediated coordination polymerization of *L*-LA, using the same solvent and catalyst, in the absence of CNTs had also an induction period of an hour. The grafted polymer content could be adjusted using reaction time, when the mole feed ratio of monomer to grafted initiator was kept constant. A control experiment was performed in which a known amount of the precursor catalyst CpTiCl<sub>2</sub>(OCH<sub>2</sub>CH<sub>3</sub>) was mixed with pristine CNTs in order to study the influence of Cp rings adsorption onto the CNTs

through  $\pi$ – $\pi$  stacking. A similar procedure as for the MWNTs-*g*-BCB-EOTiCpCl<sub>2</sub> was used for the polymerization. MWNTs were recovered after the polymerization without any polymer grafted onto it. This confirmed the absence of polymer adsorption. The polymerization of  $\epsilon$ -CL showed a similar trend as the *L*-LA while in the case of *n*-hexyl isocyanate the monomer conversion was very low (10%) even after 20 h of the polymerization.

Cai and co-workers<sup>111</sup> used MWNT–(OH)<sub>*n*</sub> for the copolymerization of *L*-lactide and  $\epsilon$ -caprolactone in the presence of stannous octanoate as the catalyst. The copolymer poly(*L*-lactide-*co*-caprolactone) nanocomposites with MWNT-*g*-poly(*L*-lactide-*co*-caprolactone) showed an increase in tensile strength, and a decrease in elastic modulus compared to the neat copolymer. The same group used MWNTs that were first functionalized with FeO<sub>4</sub>–OH for the polymerization of *L*-LA (44). The PLLA nanocomposite materials prepared with MWNTs-*g*-PLLA exhibited superparamagnetic performance, and an ability to align under low magnetic field.<sup>112</sup>

**2.2.1.5 Grafting polypeptide.** Primary amine acts as an initiator for the polymerization of cyclic aminoacids *via* *N*-carboxyanhydride (NCA) method to produce polypeptides with controlled molecular weight.<sup>113</sup> The ROP was used to graft a polypeptide from the surface of MWNTs.<sup>114</sup> Oxidized MWNTs were converted into amine functionalized MWNTs by amidation of the carboxylic groups with excess of 1,6-diaminohexane. The MWNTs–(NH<sub>2</sub>)<sub>*n*</sub> were then used for ROP of  $\gamma$ -benzyl-*L*-glutamate *N*-carboxyanhydride (BLG-NCA) (Scheme 14). The resulting hybrid material exhibited core-shell morphology with thickness of the polypeptide layer ranging from 4 to 22 nm. The thickness of the polypeptide could not be controlled by the feed ratio of NCA monomer to MWNTs–(NH<sub>2</sub>)<sub>*n*</sub>. The MWNT-*g*-(PBLG)<sub>*n*</sub> was soluble in strong polar solvents, such as DMF and dimethyl sulfoxide, and insoluble in weak polar solvents, such as acetone and esters.





**Scheme 14** Surface initiated ROP of  $\gamma$ -benzyl-L-glutamate from MWNTs.

Poly(L-lysine) is a biocompatible and biodegradable polymer and its structure facilitates various modifications, including conjugation with transferrin, epidermal growth factor, and fusogenic peptides, and thus has been widely used in the field of gene and drug delivery. Surface-initiated ROP of  $\epsilon$ -(benzyloxy-carbonyl)-L-lysine *N*-carboxyanhydride using the amine groups of the functionalized MWNTs resulted in MWNT-*g*-PLys(Z).<sup>115</sup> Acidolysis of the benzylcarbamate groups afforded water soluble MWNT-*g*-PLL. Core-shell structures were determined by high resolution TEM with the polymer shell thickness varying between 4 and 18 nm. The heterogeneous coverage of the polymer is resulting from the random distribution of amine groups on the MWNTs walls. A thicker polymer layer was observed at the bends and tips than at the straight sections.

A more detailed work involving the surface initiated ROP of BLG-NCA from amine functionalized SWNTs revealed that chemically grafted PBLG adopts a random-coil conformation in contrast to the physically adsorbed PBLG, which exhibits an  $\alpha$ -helical conformation.<sup>116</sup> It appears that intermolecular interactions of the grafted chains anchored at the one-end are not favoring the helical conformation. Microfibers of PBLG nanocomposites containing SWNT-*g*-PBLG were prepared by electrospinning. Wide-angle X-ray scattering diffractograms suggested that the SWNTs-*g*-PBLG were evenly distributed among PBLG rods in the solution and in the solid state, where PBLGs formed a short-range nematic phase inter-dispersed with amorphous domain.

**2.2.1.6 Grafting polyamide.** Anionic ROP was used by Qu *et al.*<sup>117</sup> to functionalize SWNTs with nylon-6. Nylon-6 is an important commodity polymer used in a wide variety of applications. Thus, the synthesis of nylon-functionalized carbon nanotubes is expected to improve mechanical properties.  $\epsilon$ -Caprolactam was covalently attached to the surface of the SWNT (44). The monomer grafted SWNTs were used for the polymerization of the same monomer in bulk to grow nylon-6. The nylon-6 grafted SWNTs, SWNTs-*g*-nylon-6, contained approximately 30 wt% polymer and were soluble in some organic solvents, such as formic acid and *m*-cresol.

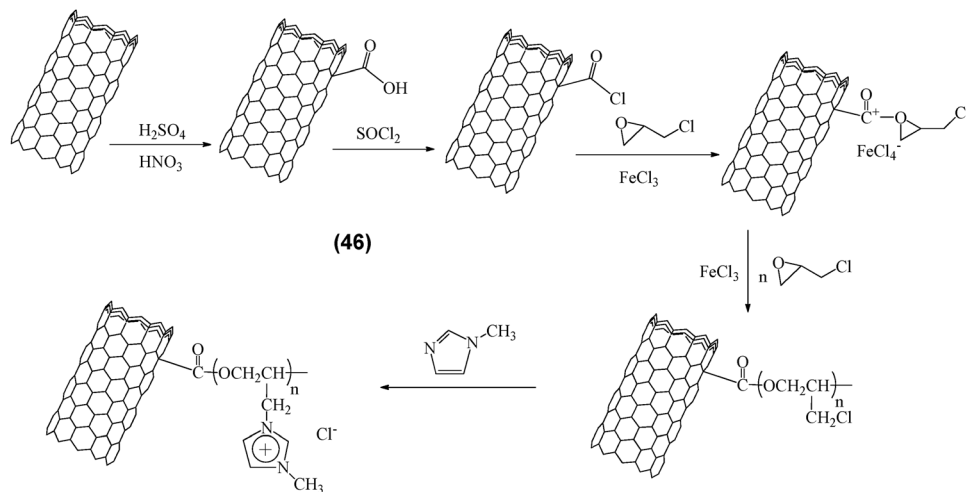
The covalent functionalization of MWNTs with nylon-6 was also reported by Adronov *et al.*<sup>118</sup> Isocyanate functionalized CNTs, prepared by reacting MWNTs-(OH)<sub>*n*</sub> with excess of toluene 2,4-diisocyanate, were used as an initiator in anionic ROP of  $\epsilon$ -caprolactam, in the presence of a sodium caprolactamate catalyst (45). A series of polymerizations was performed in order to investigate the effect of reaction time and feed ratio

(monomer/MWNT initiator) on the grafting efficiency ( $f_{wt\%}$ ). Results indicated an increase of the  $f_{wt\%}$  with polymerization time, reaching a limiting value after 6 h and was only roughly controlled by adjusting the monomer to initiator feed ratio within the range between 150 and 800.

Polyamide 6 (PA6) was grafted from MWNTs by Yan *et al.*<sup>119</sup> in a two-step process. Initially, MWNTs were covalently functionalized with copolymer (styrene-maleic anhydride) (SMA). In the second step *in situ* anionic ROP was used for the polymerization of  $\epsilon$ -caprolactam activated by the maleic anhydride groups from the grafted polymer on the MWNTs. The MWNT-*g*-PA6 was homogeneously dispersible in organic solvents such as formic acid and could melt when mixed with  $\epsilon$ -caprolactam. In a related study, by the same group, a similar grafting was performed using toluene 2,4-diisocyanate (TDI) functionalized MWNTs.<sup>120</sup>

**2.2.2 Cationic ring-opening polymerization.** The hydroxyl groups of CNTs have been used to polymerize 3-ethyl-3-(hydroxymethyl)-oxetane (EHOX) *via* cationic ring opening polymerization (CROP). The growth of hyperbranched polymer from EHOX produces numerous hydroxy groups on the surface of CNTs that can be used for further functionalization to produce nanomaterials and nanodevices. Xu *et al.*<sup>121</sup> employed cationic ROP to grow multi-hydroxy dendritic chains from the surface of the MWNTs. Hydroxy-functionalized MWNTs, in the presence of BF<sub>3</sub> Et<sub>2</sub>O, were used as initiators for the *in situ* cationic ROP of EHOX. The product was filtered and washed several times with methanol to ensure that no ungrafted polymer was adsorbed onto the MWNTs. The produced hyperbranched polyether grafted MWNTs (MWNTs-*g*-HP) were dispersible in polar solvents such as methanol, ethanol, DMF and DMSO. The amount of polymer grafted onto the surface of the MWNTs was controllable, allowing grafting up to 87 wt%. The molecular weight and the thickness of the HP on the MWNTs increased with increasing the feed ratio of monomer to macro-initiator. Free HPs resulting from the self-initiation of EHOX with BF<sub>3</sub> Et<sub>2</sub>O were removed by successive filtration and washing procedures. The degree of branching (DB-parameter), which depends on the number of dendritic, linear and terminal units of the hyperbranched polymer, was determined with <sup>13</sup>C NMR. It was found that an increase in the  $M_w$  of the grafted HPs results in a dramatic increase of the DB. Interestingly, the DB and the polydispersity index of the grafted HPs were lower than that of the HPs formed *via* self-initiation, although grafted HPs had a higher  $M_n$ . TEM indicated that the polymer shell thickness around the CNTs, in some regions, was uniform. At this point, it should be noted that the initiator functionality is distributed non-uniformly on the surface.





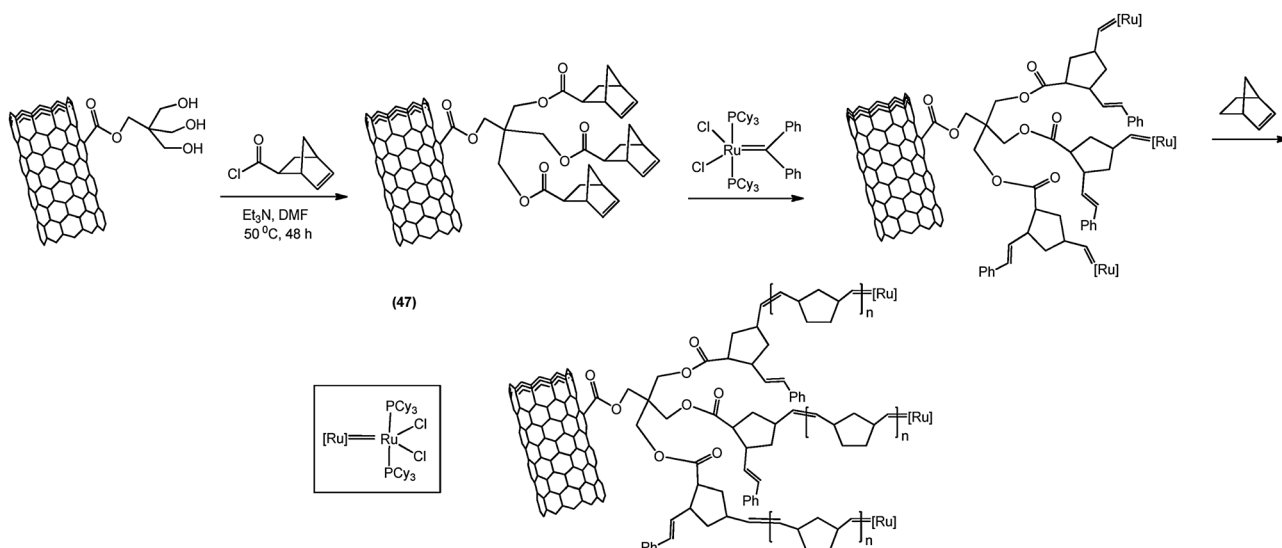
**Scheme 15** Synthetic route of the poly(epoxychloropropane)-grafted and methylimidazolium tethered MWNTs.

*In situ* cationic ROP along with quaternization reactions has been employed to embed ferricyanide onto MWNTs, in order to prepare an integrated and nanostructured electrochemical biosensor. The strategy, demonstrated by Xiang *et al.*,<sup>122</sup> was based on the introduction of positively charged functionality onto CNTs by first grafting polyether bearing alkyl halide (*via* an *in situ* cationic ROP of epichlorohydrin) and then quaternization with methylimidazole (Scheme 15). The ammonium cations on the CNTs were electrostatically complexed with ferricyanide anions  $[\text{Fe}(\text{CN})_6]^{3-}$  to form an efficient electronic transducer, due to the good electrochemical property of  $[\text{Fe}(\text{CN})_6]^{3-}$  for shuttling the electron transfer of many kinds of redox enzymes and proteins. The produced electrochemical biosensors displayed a good stability and excellent electrochemical properties.

**2.2.3 Metathesis ring-opening polymerization.** Ring opening metathesis polymerization (ROMP) of cyclic monomers has

attracted great attention recently.<sup>123</sup> However, less attention has been paid on grafting of polymer from CNTs, using this technique.

Liu and Adronov<sup>124</sup> have grafted polynorbornene brushes using ROMP from SWNTs. Multiple hydroxyl functionalized SWNTs were first reacted with norbornene acid chloride. The norbornene functionalized SWNTs were then reacted with a ruthenium based olefin metathesis catalyst to achieve covalent bonding to SWNTs. The SWNTs-*g*-(ruthenium catalyst)<sub>x</sub> were effectively used for the ROMP of norbornene (Scheme 16). The molecular weights of the grafted polymers increased linearly with polymerization time, while the polydispersity indices of the cleaved polymers were almost stable and close to 2.0. AFM images of SWNTs-*g*-polynorbornene revealed an inhomogeneous polymer growth on the surface of the SWNTs. In some cases, most of the polymer chains seemed to grow only from the tips of the SWNTs, while in others, a more uniform polymer coating around the SWNTs was observed.



**Scheme 16** Surface initiated ROMP of norbornene from MWNTs.

### 3 Conclusion

Several controlled polymerization methodologies, including radical (ATRP, NMP, and RAFT), ring-opening, and ionic (anionic and cationic) polymerizations, have been used to initiate vinyl and cyclic monomers from the surface of CNTs. Oxidatively generated acid groups on the surface of CNTs have been used to covalently react with the precursor initiator for the polymerization. Direct reactions onto the  $sp^2$  carbons (*i.e.*, 1,3-dipolar cycloaddition, Diels–Alder cycloaddition, *etc.*) have also been used for the initiator attachment. Homopolymers and diblock copolymers, V-shaped as well as dendrimers have been grafted onto all types of CNTs. The overall control of the molecular weight of the grafted polymer in the SIP has been shown *via* an increase in the wt% of polymer on the CNTs with respect to the polymerization time. Polymers in the range of 5–98 wt% have been grafted onto the CNTs. Polymer grafted CNTs, CNTs-g-polymers, are dispersible in organic solvents and have been used in the preparation of nano-composites and in sensor applications.

Even though the polymerization techniques that have been employed promise control over molecular weights, narrow MWD, and composition homogeneity, it seems that we are still far from this accomplishment. Characterization of the grafted chains after they are cleaved from the surface shows high molecular weights and broad MWDs indicating inefficient control of SIP from CNTs. Thus, the control of grafting density and average molecular weight of the grafted polymer in CNTs-g-polymers is still difficult to achieve precisely. In several reports, the grafted-polymer layer thickness on the CNTs is as high as  $\sim 25$  nm, which is very high and not correlatable, when compared to the molecular weight and the size ( $2 \times R_g$ ) of the cleaved chains from the surface. Quantitative identification of polymer layer and its conformation on the surface of CNTs are difficult. These problems are attributed to heterogeneous and inefficient grafting reactions arising from the multiple length, diameter, and functionality distributions of CNTs. Thus, the availability of a narrow distribution of SWNTs and MWNTs is essential to offer similar reactivity and efficiency for the controlled grafting of initiator and for the surface initiated polymerization. The achievements in the area of surface initiated covalent polymer grafting from CNTs, thus far obtained, will pave a way to develop new methods and processes for applications of CNTs-g-polymer materials in various fields.

### References

- 1 S. Iijima, *Nature*, 1991, **354**, 56.
- 2 C. A. Cooper, R. J. Young and M. Halsall, *Composites. Part A*, 2001, **32A**, 401.
- 3 G. Gao, T. Cagin and W. A. Goddard, *Nanotechnology*, 1998, **9**, 184.
- 4 R. Andrews and M. C. Weisenberger, *Curr. Opin. Solid State Mater. Sci.*, 2004, **8**, 31.
- 5 Z. Spitalsky, D. Tasis, K. Papagelis and C. Galiotis, *Prog. Polym. Sci.*, 2010, **35**, 357.
- 6 C. Fabbro, H. Ali-Boucetta, T. Da Ros, K. Kostarelos, A. Bianco and M. Prato, *Chem. Commun.*, 2012, **48**, 3911.
- 7 P. M. Ajayan, O. Stephan, C. Colliex and D. Trauth, *Science*, 1994, **265**, 1212.
- 8 D. Tasis, N. Tagmatarchis, A. Bianco and M. Prato, *Chem. Rev.*, 2006, **106**, 1105.
- 9 N. Karousis, N. Tagmatarchis and D. Tasis, *Chem. Rev.*, 2010, **110**, 5366.
- 10 K. Matyjaszewski and J. H. Xia, *Chem. Rev.*, 2001, **101**, 2921.
- 11 W. A. Braunecker and K. Matyjaszewski, *Prog. Polym. Sci.*, 2007, **32**, 93.
- 12 M. Ouchi, T. Terashima and M. Sawamoto, *Chem. Rev.*, 2009, **109**, 4963.
- 13 J. Pyun, T. Kowalewski and K. Matyjaszewski, *Macromol. Rapid Commun.*, 2003, **24**, 1043.
- 14 S. Edmondson, V. L. Osborne and W. T. S. Huck, *Chem. Soc. Rev.*, 2004, **33**, 14.
- 15 R. Babey, L. Lavanant, D. Paripovic, N. Schuwer, C. Sugnaux, S. Tugulu and H.-A. Klok, *Chem. Rev.*, 2009, **109**, 5437.
- 16 Z. Yao, N. Braidy, G. Botton and A. Adronov, *J. Am. Chem. Soc.*, 2003, **125**, 16015.
- 17 S. Qin, D. Qin, W. T. Ford, D. E. Resasco and J. E. Herrera, *J. Am. Chem. Soc.*, 2004, **126**, 170.
- 18 H. Kong, C. Gao and D. Yan, *J. Am. Chem. Soc.*, 2004, **126**, 412.
- 19 D. Baskaran, J. W. Mays and M. S. Bratcher, *Angew. Chem., Int. Ed.*, 2004, **43**, 2138.
- 20 S. L. Cahill, Z. Yao, A. Adronov, J. Penner, K. R. Moonosawmy, P. Kruse and G. R. Goward, *J. Phys. Chem. B*, 2004, **108**, 11412.
- 21 A. G. Rinzler, J. Liu, H. Dai, P. Nikolaev, C. B. Huffman, F. J. Rodriguez-Macias, P. J. Boul, A. H. Lu, D. Heymann, D. T. Colbert, R. S. Lee, J. E. Fischer, A. M. Rao, P. C. Eklund and R. E. Smalley, *Appl. Phys. A: Mater. Sci. Process.*, 1998, **67**, 29.
- 22 S. Qin, D. Qin, W. T. Ford, D. E. Resasco and J. E. Herrera, *Macromolecules*, 2004, **37**, 752.
- 23 D. M. Guldi, G. M. A. Rahman, S. Qin, M. M. Tchoul, W. T. Ford, M. Marcaccio, D. Paolucci, F. Paolucci, S. Campidelli and M. Prato, *Chem.–Eur. J.*, 2006, **12**, 2152.
- 24 D. M. Guldi, G. M. Aminur Rahman, J. Ramey, M. Marcaccio, D. Paolucci, F. Paolucci, S. Qin, W. T. Ford, D. Balbinot, N. Jux, N. Tagmatarchis and M. Prato, *Chem. Commun.*, 2004, **40**, 2034.
- 25 G. M. Aminur Rahman, A. Troeger, V. Sgobba, D. M. Guldi, N. Jux, D. Balbino, M. N. Tchoul, W. T. Ford, A. Mateo-Alonso and M. Prato, *Chem.–Eur. J.*, 2008, **14**, 8837.
- 26 H. Kong, C. Gao and D. Yan, *Macromolecules*, 2004, **37**, 4022.
- 27 J. H. Choi, S. B. Oh, J. Chang, I. Kim, C.-S. Ha, B. G. Kim, H. J. Han, S.-W. Joo, G.-H. Kim and H.-J. Paik, *Polym. Bull.*, 2005, **55**, 173.
- 28 T. Matrab, J. Chancelon, M. M. L'hermite, J. N. Rouzaoud, G. Deniau, J. P. Boudou, M. M. Chehimi and M. Delamar, *Colloids surf., A*, 2006, **287**, 217.
- 29 J. Albuerné, A. Boshetti-de-Fierro and V. Abetz, *J. Polym. Sci., Part B: Polym. Phys.*, 2010, **48**, 1035.
- 30 M. Liu, Y. Yang, T. Zhu and Z. Liu, *J. Phys. Chem. C*, 2007, **111**, 2379.

- 31 M. Liu, T. Zhu, Z. Li and Z. Liu, *J. Phys. Chem. C*, 2009, **113**, 9670.
- 32 H. Kong, W. Li, C. Gao, D. Yan, Y. Jin, D. R. M. Walton and H. W. Kroto, *Macromolecules*, 2004, **37**, 6683.
- 33 T. Sun, H. Liu, W. Song, X. Wang, L. Jiang, L. Li and D. Zhu, *Angew. Chem., Int. Ed.*, 2004, **34**, 4663.
- 34 R. Narain, A. Housni and L. Lane, *J. Polym. Sci., Part A: Polym. Chem.*, 2006, **44**, 6558.
- 35 L. Zhu, Q. Jin, J. Xu, J. Ji and J. Shen, *J. Appl. Polym. Sci.*, 2009, **113**, 351.
- 36 G. Romero, I. Estrela-Lopis, P. Castro-Hartmann, E. Rojas, I. Llarena, D. Sanz, E. Donath and S. E. Moya, *Soft Matter*, 2011, **7**, 6883.
- 37 X. Pei, Y. Xia, W. Liu, B. Yu and J. Hao, *J. Polym. Sci., Part A: Polym. Chem.*, 2008, **46**, 7225.
- 38 B. Fragneaud, K. Masenelli-Varlot, A. Gonzalez-Montiel, M. Terrones and J. Y. Cavaille, *Chem. Phys. Lett.*, 2006, **419**, 567.
- 39 B. Fragneaud, K. Varlot, A. G. Montiel, M. Terrones and J. V. Cavaille, *Chem. Phys. Lett.*, 2007, **444**, 1.
- 40 S. Munirasu, J. Albuerne, A. Boschetti-de-Fierro and V. Abetz, *Macromol. Rapid Commun.*, 2010, **31**, 574.
- 41 J.-T. Sun, L.-Y. Zhao, C.-Y. Hong and C.-Y. Pan, *Chem. Commun.*, 2011, **47**, 107.
- 42 H. Kong, P. Luo, C. Gao and D. Yan, *Polymer*, 2005, **46**, 2472.
- 43 C. Gao, W. Li, H. Morimoto, Y. Nagaoka and T. Maekawa, *J. Phys. Chem. B*, 2006, **110**, 7213.
- 44 H. Kong, C. Gao and D. Yan, *J. Mater. Chem.*, 2004, **14**, 1401.
- 45 A. M. Shanmugharaj, J. H. Bae, R. R. Nayak and S. H. Ryu, *J. Polym. Sci., Part A: Polym. Chem.*, 2007, **45**, 460.
- 46 W. Wu, N. V. Tsarevsky, J. L. Hudson, J. M. Tour, K. Matyjaszewski and T. Kowalewski, *Small*, 2007, **10**, 1803.
- 47 J. Ryu, B. Ramaraj and K. R. Yoon, *Surf. Interface. Anal.*, 2009, **41**, 303.
- 48 H. S. Shi, B. X. Yang, K. P. Pramoda and S. H. Goh, *Nanotechnology*, 2007, **18**, 375704.
- 49 C. L. Chochos, A. A. Stefopoulos, S. Campidelli, M. Prato, V. G. Gregoriou and J. K. Kallitsis, *Macromolecules*, 2008, **41**, 1825.
- 50 T. Hu, H. Xie, L. Chen, G. Zhong and H. Zhang, *Polym. Int.*, 2011, **60**, 93.
- 51 A. E. Daugaard, K. Jankova, J. Bogelund, J. K. Nielsen and S. Hvilsted, *J. Polym. Sci., Part A: Polym. Chem.*, 2010, **48**, 4594.
- 52 Q. Xiao, S. He, L. Liu, X. Guo, K. Shi, Z. Du and B. Zhang, *Compos. Sci. Technol.*, 2008, **68**, 321.
- 53 T. J. Aitchison, M. Ginik-Markovic, M. Saunders, P. Fredericks, S. Valiyaveetil, J. G. Matisons and G. P. Simon, *J. Polym. Sci., Part A: Polym. Chem.*, 2011, **49**, 4283.
- 54 C. Gao, *Macromol. Rapid Commun.*, 2006, **27**, 841.
- 55 W. Li, C. Gao, H. Qian, J. Ren and D. Yan, *J. Mater. Chem.*, 2006, **16**, 1852.
- 56 I. Llarena, G. Romero, R. F. Ziolo and S. E. Moya, *Nanotechnology*, 2010, **21**, 055605.
- 57 C. Gao, D. C. Vo, Y. Z. Jin, W. Li and S. P. Armes, *Macromolecules*, 2005, **38**, 8634.
- 58 Y. Zhang, H. He and C. Gao, *Macromolecules*, 2008, **41**, 9581.
- 59 Y.-L. Liu and W.-H. Chen, *Macromolecules*, 2007, **40**, 8881.
- 60 D. Priftis, G. Sakellariou, D. Baskaran, J. W. Mays and N. Hadjichristidis, *Soft Matter*, 2009, **5**, 4272.
- 61 C.-Y. Hong, Y.-Z. You, D. Wu, Y. Liu and C.-Y. Pan, *Macromolecules*, 2005, **38**, 2606.
- 62 C. Gao, S. Muthukrishnan, W. Li, J. Yuan, Y. Xu and A. H. E. Muller, *Macromolecules*, 2007, **40**, 1803.
- 63 J. Chiefari, Y. K. Chong, F. Ercole, J. Krstina, J. Jeffery, T. P. T. Le, R. T. A. Mayadunne, G. F. Meijs, C. L. Moad, G. Moad, E. Rizzardo and S. H. Thang, *Macromolecules*, 1998, **31**, 5559.
- 64 C. L. McCormack and A. B. Lowe, *Acc. Chem. Res.*, 2004, **37**, 312.
- 65 M. H. Stenzel, *Macromol. Rapid Commun.*, 2009, **30**, 1603.
- 66 J. Cui, W. P. Wang, Y. You, C. Liu and P. F. Wang, *Polymer*, 2004, **45**, 8717.
- 67 C.-Y. Hong, Y.-Z. You and C.-Y. Pan, *Polymer*, 2006, **47**, 4300.
- 68 C.-Y. Hong, Y.-Z. You and C.-Y. Pan, *Chem. Mater.*, 2005, **17**, 2247.
- 69 G. Xu, W.-T. Wu, Y. Wang, W. Pang, P. Wang, Q. Zhu and F. Lu, *Nanotechnology*, 2006, **17**, 2458.
- 70 G. Xu, W. T. Wu, Y. Wang, W. Pang, P. Wang, Q. Zhu and P. Wang, *Nanotechnology*, 2007, **18**, 145606.
- 71 G. Xu, Y. Wang, W. Pang, W. T. Wu, Q. Zhu and P. Wang, *Polym. Int.*, 2007, **56**, 847.
- 72 G. Xu, W.-T. Wu, Y. Wang, W. Pang, Q. Zhu, P. Wang and Y. You, *Polymer*, 2006, **47**, 5909.
- 73 Y.-Z. You, C.-Y. Hong and C.-Y. Pan, *Nanotechnology*, 2006, **17**, 2350.
- 74 C.-Y. Hong, Y.-Z. You and C.-Y. Pan, *J. Polym. Sci., Part A: Polym. Chem.*, 2006, **44**, 2419.
- 75 X. Pei, J. Hao and W. Liu, *J. Phys. Chem. C*, 2007, **111**, 2947.
- 76 X. Pei, W. Liu and J. Hao, *J. Polym. Sci., Part A: Polym. Chem.*, 2008, **46**, 3014.
- 77 G. J. Wang, S. Z. Huang, Y. Wang, L. L. Liu, J. Qiu and Y. Li, *Polymer*, 2007, **48**, 728.
- 78 B. Zhang, J. Wang, Y. Chen, D. Fruchtl, B. Yu, X. Zhuang, N. He and W. J. Blau, *J. Polym. Sci., Part A: Polym. Chem.*, 2010, **48**, 3161.
- 79 C. J. Hawker, A. W. Bosman and E. Harth, *Chem. Rev.*, 2001, **101**, 3661.
- 80 M. Dehonor, K. Masenelli-Varlot, A. Gonzalez-Montiel, C. Gauthier, J. Y. Cavaille, H. Terrones and M. Terrones, *Chem. Commun.*, 2005, **41**, 5349.
- 81 X. Zhao, W. Lin, N. Song, X. Chen, X. Fan and Q. Zhou, *J. Mater. Chem.*, 2006, **16**, 4619.
- 82 X.-D. Zhao, X.-H. Fan, X.-H. Chen, C.-P. Chai and Q.-F. Zhou, *J. Polym. Sci., Part A: Polym. Chem.*, 2006, **44**, 4656.
- 83 D.-Q. Fan, J.-P. He, W. Tang, J.-T. Xu and Y.-L. Yang, *Eur. Polym. J.*, 2007, **43**, 26.
- 84 J. H. Chang, Y. W. Lee, B. G. Kim, H.-K. Kim, I. S. Choi and H.-J. Paik, *Compos. Interfaces*, 2007, **14**, 493.
- 85 N. Hadjichristidis, M. Pitsikalis, S. Pispas and H. Iatrou, *Chem. Rev.*, 2001, **101**, 3747.
- 86 G. Viswanathan, N. Chakrapani, H. Yang, B. Wei, H. Chung, K. Cho, C. Y. Ryu and P. M. Ajayan, *J. Am. Chem. Soc.*, 2003, **125**, 9258.

- 87 S. Chen, D. Chen and G. Wu, *Macromol. Rapid Commun.*, 2006, **27**, 882.
- 88 F. Liang, K. Beach, A. K. Sadana, Y. I. Cantu, J. M. Tour and W. E. Billups, *Chem. Mater.*, 2006, **18**, 4764.
- 89 G. Sakellariou, H. Ji, J. W. Mays and D. Baskaran, *Chem. Mater.*, 2008, **20**, 6217.
- 90 D. Baskaran, G. Sakellariou, J. W. Mays and M. S. Bratcher, *J. Nanosci. Nanotechnol.*, 2007, **7**, 1560.
- 91 G. Sakellariou, H. Ji, J. W. Mays, N. Hadjichristidis and D. Baskaran, *Chem. Mater.*, 2007, **19**, 6370.
- 92 N. Kamber, W. Jeong, R. M. Waymouth, R. C. Pratt, B. G. G. Lohmeijer and J. L. Hedrick, *Chem. Rev.*, 2007, **107**, 5813.
- 93 K. R. Yoon, W. J. Kim and I. S. Choi, *Macromol. Chem. Phys.*, 2004, **205**, 1218.
- 94 L. Zhou, C. Gao and W. Xu, *Macromol. Chem. Phys.*, 2009, **210**, 1011.
- 95 M. Adeli, N. Mirab, M. S. Alavidjeh, Z. Sobhani and F. Atyabi, *Polymer*, 2009, **50**, 3528.
- 96 C. Gao, H. He, L. Zhou, X. Zheng and Y. Zhang, *Chem. Mater.*, 2009, **21**, 360.
- 97 J. Ma, X. Cheng, X. Ma, S. Deng and A. Hu, *J. Polym. Sci., Part A: Polym. Chem.*, 2010, **48**, 5541.
- 98 R.-S. Lee, W.-H. Chen and J.-H. Lin, *Polymer*, 2011, **52**, 2180.
- 99 F. Buffa, H. Hu and D. Resasco, *Macromolecules*, 2005, **38**, 8258.
- 100 H. Zeng, C. Gao and D. Yan, *Adv. Funct. Mater.*, 2006, **16**, 812.
- 101 M. Castro, J. Lu, S. Bruzard, B. Kumar and J.-F. Feller, *Carbon*, 2009, **47**, 1930.
- 102 B. Ruelle, S. Peeterbroeck, R. Gouttebaron, T. Godfroid, F. Monteverde, J.-P. Dauchot, M. Alexandre, M. Hecq and P. Dubois, *J. Mater. Chem.*, 2007, **17**, 157.
- 103 Y. Yang, C. P. Tsui, C. Y. Tang, S. Qiu, Q. Zhao, X. Cheng, Z. Sun, R. K. Y. Li and X. Xie, *Eur. Polym. J.*, 2010, **46**, 145.
- 104 J. Chen, M. J. Dyer and M.-F. Yu, *J. Am. Chem. Soc.*, 2001, **123**, 6201.
- 105 D. Priftis, G. Sakellariou, N. Hadjichristidis, E. K. Penott, A. T. Lorenzo and A. J. Muller, *J. Polym. Sci., Part A: Polym. Chem.*, 2009, **47**, 4379.
- 106 D. Priftis, G. Sakellariou, J. W. Mays and N. Hadjichristidis, *J. Polym. Sci., Part A: Polym. Chem.*, 2010, **48**, 1104.
- 107 G.-X. Chen, H. S. Kim, B. H. Park and J.-S. Yoon, *Macromol. Chem. Phys.*, 2007, **208**, 389.
- 108 H.-S. Kim, B. H. Park, J.-S. Yoon and H.-J. Jin, *Eur. Polym. J.*, 2007, **43**, 1729.
- 109 H.-S. Kim, Y. S. Chae, B. H. Park, J.-S. Yoon, M. Kang and H.-J. Jin, *Curr. Appl. Phys.*, 2008, **8**, 803.
- 110 D. Priftis, N. Petzetakis, G. Sakellariou, M. Pitsikalis, D. Baskaran, J. W. Mays and N. Hadjichristidis, *Macromolecules*, 2009, **42**, 3340.
- 111 A. N. Chakoli, J. Wan, J. T. Feng, M. Amirian, J. H. Sui and W. Cai, *Appl. Surf. Sci.*, 2009, **256**, 170.
- 112 J. Feng, W. Cai, J. Sui, Z. Li, J. Wan and A. N. Chakoli, *Polymer*, 2008, **49**, 4989.
- 113 N. Hadjichristidis, H. Iatrou, M. Pitsikalis and G. Sakellariou, *Chem. Rev.*, 2009, **109**, 5528.
- 114 Y. Yao, W. Li, S. Wang, D. Yan and X. Chen, *Macromol. Rapid Commun.*, 2006, **27**, 2019.
- 115 J. Li, W.-D. He, L.-P. Yang, X.-L. Sun and Q. Hua, *Polymer*, 2007, **48**, 4352.
- 116 H. Tang and D. Zhang, *J. Polym. Sci., Part A: Polym. Chem.*, 2010, **48**, 2340.
- 117 L. Qu, M. L. Veca, Y. Lin, A. Kitaygorodisky, B. Chen, M. A. McCall, J. W. Connell and Y. P. Sun, *Macromolecules*, 2005, **38**, 10328.
- 118 M. Yang, Y. Gao, H. Li and A. Adronov, *Carbon*, 2007, **45**, 2327.
- 119 D. Yan and G. Yang, *Mater. Lett.*, 2009, **63**, 298.
- 120 D. Yan and G. Yang, *J. Appl. Polym. Sci.*, 2009, **112**, 3620.
- 121 Y. Xu, C. Gao, H. Kong, D. Yan, Z. Y. Jin and P. C. P. Watts, *Macromolecules*, 2004, **37**, 8846.
- 122 L. Xiang, Z. Zhang, P. Yu, J. Zhang, L. Su, T. Ohsaka and L. Mao, *Anal. Chem.*, 2008, **80**, 6587.
- 123 C. W. Bielawski and R. H. Grubbs, *Prog. Polym. Sci.*, 2007, **32**, 1.
- 124 Y. Liu and A. Adronov, *Macromolecules*, 2004, **37**, 4755.